Electromagnetic wave propagation in dispersive and complex material with time domain techniques

Kristensson, Gerhard; Karlsson, Anders; Rikte, Sten

2000

CODEN:LUTEDX/(TEAT-7086)/1-38/(2000)

Electromagnetic wave propagation in dispersive and complex material with time domain techniques

Gerhard Kristensson, Anders Karlsson, and Sten Rikte

Department of Electroscience
Electromagnetic Theory
Lund Institute of Technology
Sweden

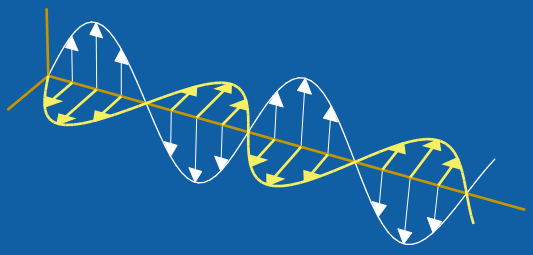

Gerhard Kristensson, Anders Karlsson, and Sten Rikte

Department of Electroscience
Electromagnetic Theory
Lund Institute of Technology
P.O. Box 118
SE-221 00 Lund
Sweden

Editor: Gerhard Kristensson

Abstract

In this paper a time domain formulation of the first and second precursor in a dispersive materials is reviewed. These precursors are determined by the susceptibility kernel of the medium, which characterizes the medium in a time domain formulation. The propagator operators of the fields are corner stones in the formulation. These operators are then approximated by a pertinent factorization procedure that defines to the first and second precursors of the medium. Wave propagation in a biisotropic medium is also treated and the early time behavior of a transient signal is addressed. A series of numerical examples illustrates the theory.

1 Introduction

All materials exhibit dispersion to some extent. The effects of dispersion in a given material depends on the temporal behavior of the propagating wave and the distance the wave travels. There are applications where dispersion can be neglected, but in most cases it is not appropriate to neglect it. In linear classical electrodynamics most materials can be characterized as Debye type materials or Lorentz type materials, see [11]. The Debye type is appropriate for polar liquids in the microwave regime and is due to the rotational motion of the molecules. This is for instance the explanation why water gets hot in microwave ovens. Most other materials are of the Lorentz type. Lorentz' model is based on the motion of bounded charges and leads to a system with one or several resonant frequencies.

The basic results for wave propagation in dispersive materials were obtained by frequency domain methods and were presented by Sommerfeld [29] and Brillouin [3] in two consecutive articles under the same title in *Annalen der Physik* in 1914. They used saddle-point methods to obtain the asymptotic behavior of a wave that has traveled a (comparatively) large distance in a single resonance Lorentz material. They showed that the asymptotic behavior is determined by two wave phenomena which they referred to as forerunners or precursors. The first precursor (Sommerfeld's precursor) determines the early time behavior of the wave and is due to a saddle point for high frequencies. The second precursor is due to a saddle point close to the origin in the frequency plane and it propagates with the group velocity at zero frequency. The results of Brillouin and Sommerfeld have been much refined and generalized by Oughstun and Sherman. Their results are summarized in [23].

In this chapter a time-domain technique for wave propagation in dispersive materials is discussed. The method is based upon a wave splitting technique and the concept of propagators. The wave splitting is a method for decoupling hyperbolic equations into one-way wave equations. This is always possible in a homogeneous medium. The propagation of the solutions to the one-way equations in this chapter is described by operators referred to as propagators. The propagators map a split field from one position in the material to another position. In homogeneous materials the propagators are obtained very efficiently by numerically solving Volterra integral equations. With the fast computers of today it is possible to solve the pre-

cursors from the Volterra equation to such depths where the asymptotic results are valid even for complicated materials.

The wave splitting is used extensively in wave propagation methods. The simplest form of it is the well-known d'Alembert solution to the wave equation for linear, homogeneous, isotropic, non-dispersive materials. The wave splitting can be performed for other types of materials and we show how it is obtained in isotropic and bi-isotropic dispersive media. The propagator method is closely related to the imbedding method and the Green function method that have been applied to large classes of direct and inverse scattering problems. A review of these methods is given in a recent publication [10].

2 Modeling of linear materials

The Maxwell equations are the basic equations for modeling the dynamics of the fields in macroscopic electromagnetic applications.

$$\begin{cases} \nabla \times \boldsymbol{E}(\boldsymbol{r},t) = -\dfrac{\partial}{\partial t}\boldsymbol{B}(\boldsymbol{r},t) \\ \nabla \times \boldsymbol{H}(\boldsymbol{r},t) = \boldsymbol{J}(\boldsymbol{r},t) + \dfrac{\partial}{\partial t}\boldsymbol{D}(\boldsymbol{r},t) \end{cases} \tag{2.1}$$

Here, the electric and the magnetic fields are denoted by $\boldsymbol{E}$ and $\boldsymbol{H}$, respectively, and the electric and the magnetic flux densities are denoted by $\boldsymbol{D}$ and $\boldsymbol{B}$, respectively. The current density is denoted $\boldsymbol{J}$.

The constitutive relations model the dynamics of the charged constituents of the materials. Under the assumption of linear response to the applied fields, causality, invariance under time translations, and continuity, these constitutive relations have the following general form [12]:

$$\begin{cases} c_0\eta_0\boldsymbol{D}(\boldsymbol{r},t) = \boldsymbol{\epsilon}\cdot\boldsymbol{E}(\boldsymbol{r},t) + (\boldsymbol{\chi}_{\mathrm{ee}} * \boldsymbol{E})(\boldsymbol{r},t) \\ \qquad\qquad + \eta_0\boldsymbol{\xi}\cdot\boldsymbol{H}(\boldsymbol{r},t) + \eta_0(\boldsymbol{\chi}_{\mathrm{em}} * \boldsymbol{H})(\boldsymbol{r},t) \\ c_0\boldsymbol{B}(\boldsymbol{r},t) = \boldsymbol{\zeta}\cdot\boldsymbol{E}(\boldsymbol{r},t) + (\boldsymbol{\chi}_{\mathrm{me}} * \boldsymbol{E})(\boldsymbol{r},t) \\ \qquad\qquad + \eta_0\boldsymbol{\mu}\cdot\boldsymbol{H}(\boldsymbol{r},t) + \eta_0(\boldsymbol{\chi}_{\mathrm{mm}} * \boldsymbol{H})(\boldsymbol{r},t) \end{cases}$$

where $c_0 = 1/\sqrt{\epsilon_0\mu_0}$ is the speed of light in vacuum, $\eta_0 = \sqrt{\mu_0/\epsilon_0}$ is the wave impedance in vacuum, and ϵ_0 and μ_0 are the permittivity and permeability of vacuum, respectively. We refer to these expressions as constitutive relations for a bi-anisotropic medium. Here, the star symbol $*$ denotes temporal convolution with a scalar (dot) product included, *i.e.*,

$$(\boldsymbol{\alpha} * \boldsymbol{B})(\boldsymbol{r},t) = \int_{-\infty}^{t} \boldsymbol{\alpha}(t-t')\cdot\boldsymbol{B}(\boldsymbol{r},t')\,dt'$$

Dispersion is modeled by four time-dependent, dyadic-valued susceptibility kernels $\boldsymbol{\chi}_{\mathrm{ee}}$, $\boldsymbol{\chi}_{\mathrm{em}}$, $\boldsymbol{\chi}_{\mathrm{me}}$ and $\boldsymbol{\chi}_{\mathrm{mm}}$, which vanish for $t < 0$ due to causality and, furthermore, are assumed to be bounded, smooth (infinitely differentiable), and absolutely

Type	$\boldsymbol{\epsilon}, \boldsymbol{\chi}_{\rm ee}, \boldsymbol{\mu}, \boldsymbol{\chi}_{\rm mm}$	$\boldsymbol{\xi}, \boldsymbol{\chi}_{\rm em}, \boldsymbol{\zeta}, \boldsymbol{\chi}_{\rm me}$
Isotropic	All $\sim \mathbf{I}$	Both $\mathbf{0}$
An-isotropic	Some not $\sim \mathbf{I}$	Both $\mathbf{0}$
Bi-isotropic	All $\sim \mathbf{I}$	Both $\sim \mathbf{I}$ and $\neq \mathbf{0}$
Bi-an-isotropic	All other cases	

Table 1: Classification of material w.r.t. the symmetry properties of the constitutive relations.

integrable for $t > 0$. These kernels have the dimension of frequency. Observe that an absolutely integrable susceptibility kernel vanishes in the high-frequency limit (the Riemann-Lebesgue lemma), *i.e.*,

$$\lim_{\omega\to\infty} \int_0^\infty e^{i\omega t} \boldsymbol{\chi}_{kk'}(t)\, dt = \mathbf{0} \qquad k, k' = \text{e,m}$$

The instantaneous response (optical response) of the material is modeled by the dimensionless dyadics $\boldsymbol{\epsilon}$, $\boldsymbol{\xi}$, $\boldsymbol{\zeta}$ and $\boldsymbol{\mu}$. The concept of optical response is analyzed in more detail in a separate subsection below. For simplicity we assume all dyadics $\boldsymbol{\epsilon}$, $\boldsymbol{\xi}$, $\boldsymbol{\zeta}$ and $\boldsymbol{\mu}$ to be constant and $\boldsymbol{\chi}_{\rm kk'}$, k,k' = e,m to be independent of the spatial coordinates $\boldsymbol{r}$, *i.e.*, the materials are homogeneous.

Linear materials are classified according to the symmetry properties of the dyadics $\boldsymbol{\chi}_{\rm kk'}$, k,k' = e,m and $\boldsymbol{\epsilon}$, $\boldsymbol{\xi}$, $\boldsymbol{\zeta}$ and $\boldsymbol{\mu}$. The definitions of isotropic, anisotropic, bi-isotropic, and bi-anisotropic materials, which are exclusive, are given in Table 1.

For the special case of a linear, homogeneous, isotropic material, we get

$$\begin{cases} \boldsymbol{D}(\boldsymbol{r},t) = \epsilon_0 \left(\epsilon \boldsymbol{E}(\boldsymbol{r},t) + (\chi_{\rm e} * \boldsymbol{E})\,(t)\right) \\ \boldsymbol{B}(\boldsymbol{r},t) = \mu_0 \left(\mu \boldsymbol{H}(\boldsymbol{r},t) + (\chi_{\rm m} * \boldsymbol{H})\,(\boldsymbol{r},t)\right) \end{cases} \tag{2.2}$$

This is the simplest constitutive relation of a medium with dispersion effects, and we adopt a special case of this model in the analysis of Section 3. Two explicit models for isotropic materials are important. These are the relaxation (Debye's) and the resonance (Lorentz') models, see the subsections below.

2.1 Optical response

The optical response, ϵ, present in (2.2), is a time domain model to accommodate all fast processes in the material that cannot be resolved with the variation of the applied field. To more clearly see the origin of the optical response, let the optical response be absent ($\epsilon = 1$), but assume that the susceptibility kernel $\chi_{\rm e}$ is a sum of two terms, a rapidly varying term, $\chi_{\rm f}$, and a slowly varying term $\chi_{\rm s}$. The variations of the applied field determine what is fast and what is slow in this context. For microwave applications the fast processes are infra-red and optical polarization effects in the material, while for optical applications the fast processes are ultra-violet phenomena. We thus have, suppressing spatial dependence, which is of no interest

here

$$\begin{aligned}\frac{1}{\epsilon_0}\boldsymbol{D}(t) =& \boldsymbol{E}(t) + (\chi_{\mathrm{f}} * \boldsymbol{E})(t) + (\chi_{\mathrm{s}} * \boldsymbol{E})(t)\\ \approx& \boldsymbol{E}(t) + \boldsymbol{E}(t)\int_{-\infty}^{t} \chi_{\mathrm{f}}(t-t')\,dt' + (\chi_{\mathrm{s}} * \boldsymbol{E})(t)\\ =& \epsilon\boldsymbol{E}(t) + (\chi_{\mathrm{s}} * \boldsymbol{E})(t)\end{aligned}$$

where the field $\boldsymbol{E}(t)$ has been taken outside the integration of the first integral due to the rapid variations of the kernel χ_{f}, and where $\epsilon = 1 + \int_0^\infty \chi_{\mathrm{f}}(t)\,dt$.

The optical response, which is a time-domain concept is related to the complex permittivity function $\hat{\epsilon}(\omega)$, which is defined by the Fourier transform of the susceptibility kernel, *i.e.*,

$$\hat{\epsilon}(\omega) = 1 + \int_0^\infty \chi_{\mathrm{e}}(t)\exp(i\omega t)\,dt$$

Specifically, the optical response corresponds to the low-frequency behavior of the permittivity function $\hat{\epsilon}(\omega)$, since, at $\omega = 0$ we have

$$\hat{\epsilon}(0) = 1 + \int_0^\infty \chi_{\mathrm{e}}(t)\,dt = \epsilon + \int_0^\infty \chi_{\mathrm{s}}(t)\,dt$$

and we see that the low-frequency behavior of the permittivity function is related to the optical response and the (average) properties of the susceptibility kernel. We also see that the kernel χ_{e} in (2.2) is in fact χ_{s}. If the applied field has infinite bandwidth, no optical response can be identified and $\epsilon = 1$, *i.e.*, as in vacuum. A similar discussion applies to the general, linear medium.

2.2 Relaxation model

Debye's model or the relaxation model is a useful model for polar liquids. The rate of alignment of the molecules is modeled by the frequency α and the process that tries to randomly orient the molecular polarization is modeled by the relaxation time $\tau \geq 0$. The explicit form of the electric susceptibility kernel is [16]

$$\chi_{\mathrm{e}}(t) = \alpha e^{-t/\tau}$$

and the optical response is $\epsilon = 1$. An equivalent expression for the magnetic susceptibility kernel can also be obtained, but this model is less often used in the literature.

2.3 Resonance model

Lorentz' model or the resonance model is often used as a model for the electromagnetic response in solids. Assume $\omega_0 \geq 0$ is the harmonic frequency of the restoring force, $\nu \geq 0$ is the collision frequency, and $\omega_p = \sqrt{Nq^2/\epsilon_0 m} > 0$ is the plasma frequency of the medium. The explicit form of the electric susceptibility kernel is [16]

$$\chi_{\mathrm{e}}(t) = \frac{\omega_p^2}{\nu_0} e^{-\nu t/2} \sin \nu_0 t \tag{2.3}$$

where $\nu_0^2 = \omega_0^2 - \nu^2/4$ and the optical response is $\epsilon = 1$. Just as in the Debye's model there is a magnetic susceptibility kernel in analogy to the electric one.

The relaxation and the resonance models are examples of useful models. They correspond to first and second order ODEs with constant coefficients, respectively. Generalization to higher order equations can be found in Refs. 9 and 27.

2.4 Restrictions on the constitutive relations

Since all realistic materials have losses, it is important to exploit the concept of dissipation in the material. Dissipation constrains the form of the dyadic-valued (susceptibility) functions $\boldsymbol{\chi}_{\mathrm{kk'}}$, k,k' = e,m, and the dyadics $\boldsymbol{\epsilon}$, $\boldsymbol{\xi}$, $\boldsymbol{\zeta}$ and $\boldsymbol{\mu}$. In Refs. 7 and 12 it is shown that in a passive medium the following constraints must hold:

$$\boldsymbol{\epsilon} = \boldsymbol{\epsilon}^t \qquad \boldsymbol{\xi} = \boldsymbol{\zeta}^t \qquad \boldsymbol{\mu} = \boldsymbol{\mu}^t$$

Here ^{t} denotes the transpose of the dyadic. Moreover, the following 6-dimensional dyadics

$$\begin{pmatrix} \boldsymbol{\epsilon} & \boldsymbol{\xi} \\ \boldsymbol{\zeta} & \boldsymbol{\mu} \end{pmatrix} \qquad \begin{pmatrix} \boldsymbol{\chi}_{\mathrm{ee}}(0^+) & \boldsymbol{\chi}_{\mathrm{em}}(0^+) \\ \boldsymbol{\chi}_{\mathrm{me}}(0^+) & \boldsymbol{\chi}_{\mathrm{mm}}(0^+) \end{pmatrix}$$

are positive semi-definite dyadics. Additional constraints can be found in Refs. 7, 12 and 17.

The medium is reciprocal if and only if the constitutive relations satisfy [12, 17]

$$\begin{cases} \boldsymbol{\epsilon} = \boldsymbol{\epsilon}^t \\ \boldsymbol{\xi} = -\boldsymbol{\zeta}^t \\ \boldsymbol{\mu} = \boldsymbol{\mu}^t \end{cases} \qquad \begin{cases} \boldsymbol{\chi}_{\mathrm{ee}}(t) = \boldsymbol{\chi}_{\mathrm{ee}}^t(t) \\ \boldsymbol{\chi}_{\mathrm{em}}(t) = -\boldsymbol{\chi}_{\mathrm{me}}^t(t) \\ \boldsymbol{\chi}_{\mathrm{mm}}(t) = \boldsymbol{\chi}_{\mathrm{mm}}^t(t) \end{cases}$$

We immediately conclude that all isotropic materials are reciprocal. Even though most materials are reciprocal there are important exceptions, *e.g.*, ionized materials in an external magnetic field and ferrites in an external magnetic field.

3 Isotropic, homogeneous media

For pedagogical reasons we restrict the detailed analysis to homogeneous, isotropic materials without magnetic dispersion, *i.e.*, the constitutive relations are, see (2.2)

$$\begin{cases} \boldsymbol{D}(\boldsymbol{r},t) = \epsilon_0 \left(\epsilon \boldsymbol{E}(\boldsymbol{r},t) + (\chi_{\mathrm{e}} * \boldsymbol{E})\,(\boldsymbol{r},t)\right) \\ \boldsymbol{B}(\boldsymbol{r},t) = \mu_0 \mu \boldsymbol{H}(\boldsymbol{r},t) \end{cases}$$

Some extensions of the analysis presented in this section are outlined in Section 8.

We proceed the analysis in two steps. First, in this section we investigate the solutions in an homogeneous material. Specifically, we introduce the concepts of wave splitting and of propagators. The reflection problem by a slab is then addressed in Section 7.

3.1 Dynamics

We seek one-dimensional transverse electric and magnetic (TEM) solutions of the source-free Maxwell field equations in the isotropic material. We denote the direction of propagation with z and assume the linearly polarized fields

$$\begin{cases} \boldsymbol{E}(\boldsymbol{r},t) = \boldsymbol{e}_x E(z,t) \\ \boldsymbol{H}(\boldsymbol{r},t) = \boldsymbol{e}_y H(z,t) \end{cases}$$

where $\boldsymbol{e}_x$ and $\boldsymbol{e}_y$ are the unit vectors in the x and y directions, respectively. The other generic polarization with the electric field along the y-axis gives results that are completely analogous due to the isotropy of the material. Any other polarization is then obtained by superposition.

Elimination of the flux densities in the Maxwell equations, (2.1), yields a first-order system of hyperbolic integro-differential equations in the non-vanishing electric and magnetic field components.

$$c_0 \frac{\partial}{\partial z} \begin{pmatrix} E \\ -\eta_0 H \end{pmatrix} = \frac{\partial}{\partial t} \left\{ \begin{pmatrix} 0 & \mu \\ \epsilon + \chi_{\mathrm{e}} * & 0 \end{pmatrix} \begin{pmatrix} E \\ -\eta_0 H \end{pmatrix} \right\} \tag{3.1}$$

3.2 Wave splitting

One way to deal with propagation problems in temporally dispersive media is to adopt a dispersive wave splitting [26]. We introduce new dependent variables (split fields) by

$$\begin{cases} E^+(z,t) = \dfrac{1}{2}\left(E(z,t) + \eta(1+Z*)\eta_0 H(z,t)\right) \\ E^-(z,t) = \dfrac{1}{2}\left(E(z,t) - \eta(1+Z*)\eta_0 H(z,t)\right) \end{cases} \tag{3.2}$$

where the relative high-frequency wave impedance is denoted by $\eta = \sqrt{\mu/\epsilon}$. The basic idea behind this change of dependent variables is to use a specific choice of

the kernel $Z(t)$ such that there is no interaction between the new split fields $E^{\pm}$. The new split fields satisfy one-way wave equations, and, therefore, represent the correct kinematic parts of the wave propagation problem. This is a wave splitting with respect to the dispersive background characterized by the (real-valued) optical responses ϵ, μ and the susceptibility kernel $\chi_{\rm e}(t)$.

In terms of the split fields, $E^{\pm}(z,t)$, the electric and magnetic fields are given by

$$\begin{cases} E(z,t) = E^{+}(z,t) + E^{-}(z,t) \\ \eta\eta_0 H(z,t) = (1 + N*)(E^{+}(z,t) - E^{-}(z,t)) \end{cases} \tag{3.3}$$

where the kernel $N(t)$ is uniquely determined by $Z(t)$, see below. The dispersive wave splitting (3.2)–(3.3) should be interpreted locally throughout space. In the absence of dispersion ($\chi_{\rm e} = 0$), we have

$$\begin{cases} E(z,t) = E^{+}(z,t) + E^{-}(z,t) \\ \eta\eta_0 H(z,t) = E^{+}(z,t) - E^{-}(z,t) \end{cases}$$

In the expressions (3.2)–(3.3) above, the intrinsic impedance kernel $Z(t)$ and the refractive kernel $N(t)$ vanish for $t < 0$ and are well-behaved for $t > 0$. Furthermore, $N(t)$ is the resolvent of $Z(t)$, *i.e.*,

$$N(t) + Z(t) + (N * Z)(t) = 0 \tag{3.4}$$

The aim of the dispersive wave splitting is to decouple the Maxwell equations. By differentiating (3.2) with respect to z, using (3.1) and (3.3), the coupling terms between the split fields $E^{\pm}$ both are proportional

$$\epsilon\frac{\partial}{\partial t}N * E^{\pm} - \frac{\partial}{\partial t}\chi_{\rm e} * E^{\pm} - Z * \frac{\partial}{\partial t}\left(\epsilon E^{\pm} + \chi_{\rm e} * E^{\pm}\right)$$

We require this expression to vanish for arbitrary fields E^{+} and E^{-}. This leads to the following equation for the kernel $N(t)$:

$$2N(t) + (N * N)(t) = \chi_{\rm e}(t)/\epsilon \tag{3.5}$$

This is a nonlinear Volterra integral equation of the second kind which is known to be uniquely solvable in the space of bounded and smooth functions in each bounded time interval, $0 < t < T$. Furthermore, they are numerically stable [21]. Thus, the construction of $Z(t)$ and $N(t)$ from $\chi_{\rm e}(t)$ is a well posed problem.

The one-way equations for the split fields read

$$(c\partial_z \pm \partial_t)E^{\pm} = \mp\partial_t\left(N * E^{\pm}\right) \tag{3.6}$$

where the wave front speed in the non-dispersive background is $c = c_0/\sqrt{\epsilon\mu}$. We see that the split fields E^{+} and E^{-} represent up- and down-going fields, respectively.

In summary, the unique solution $N(t)$ of the non-linear Volterra equation of the second kind (3.5) and its resolvent $Z(t)$, see equation (3.4), lead to a set of two one-way wave equations in the split fields $E^{\pm}$. We then obtain the electric and the magnetic fields by equation (3.3).

3.3 Expansion of the kernels

Using the method of successive approximation in (3.5) we can expanded the refractive kernel, $N(t)$, in a power series of temporal convolutions. This series converges in each bounded time interval, $0 < t < T$ [21].

$$N(t) = \sum_{k=1}^{\infty} \binom{\frac{1}{2}}{k} \epsilon^{-k} \left((\chi_{\mathrm{e}} *)^{k-1} \chi_{\mathrm{e}} \right)(t)$$

Similarly, we can expand the impedance kernel in a power series of temporal convolutions, see (3.4). The result is

$$Z(t) = \sum_{k=1}^{\infty} (-1)^k \left((N*)^{k-1} N \right)(t)$$

3.4 Propagators

We seek solutions to the fields $E^{\pm}$ in (3.6). These solutions can formally be written as

$$\begin{aligned} &E^{\pm}(z_2, t \pm (z_2 - z_1)/c) \\ &\quad = \left[\mathcal{P}\left(\pm (z_2 - z_1) \right) E^{\pm}(z_1, \cdot) \right](t) \end{aligned} \tag{3.7}$$

$(-\infty < z_1, z_2 < \infty)$, where the temporal integral operator $\mathcal{P}(z_2 - z_1)$ is referred to as the wave propagator of the temporally dispersive medium and t denotes wave front time, *i.e.*, the time measured from the arrival of the wave front.[1] Due to the homogeneity of the material the propagator is invariant under spatial translations, and, therefore, the propagator $\mathcal{P}$ is a function of $z_2 - z_1$, *i.e.*, $\mathcal{P}\left(\pm (z_2 - z_1) \right)$. The interpretation of the spatial argument is that $z_1 \leq z_2$ corresponds to propagation of up-going or down-going fields upwards. The other case, $z_2 \leq z_1$ corresponds to propagation of up-going or down-going fields downwards.

The dynamic equations (3.6) show that the wave propagator satisfies the operator identity

$$\begin{cases} \partial_z \mathcal{P}(z) = -\mathcal{K}\mathcal{P}(z) \\ \mathcal{P}(0) = 1 \end{cases} \tag{3.8}$$

where the temporal integral operator $\mathcal{K}$ is related to the wave number of the dispersive medium as

$$\begin{cases} \mathcal{K} = \dfrac{1}{c}\partial_t N* = \dfrac{1}{c}N(0) + K* \\ K(t) = \dfrac{1}{c}N'(t) \end{cases} \tag{3.9}$$

[1] Notice the difference between the real physical time t and wave front time τ related by $\tau = t - z/c$. We use the same letter t for both real time and wave front time in the text. From the context it is obvious which time we refer to.

The wave propagator is closely related to the causal fundamental solution of the dispersive wave operator, see [13].

The formal solution to (3.8) is

$$\mathcal{P}(z) = \exp\left(-z\mathcal{K}\right) \tag{3.10}$$

where the exponential of an operator is defined by its Taylor series expansion. Multiplication by the time-shift operator[2]

$$\mathcal{P}_0(z) = \exp\left(-zc^{-1}\partial_t\right) = \delta(\cdot - z/c) *$$

gives a wave propagator, $\mathcal{P}_0(z)\mathcal{P}(z)$, defined in terms of real physical time.[3]

Two-fold application of (3.7) (or use (3.10)) shows that the wave propagator, $\mathcal{P}(z)$, satisfies the relations

$$\begin{cases} \mathcal{P}(z_1 + z_2) = \mathcal{P}(z_1)\mathcal{P}(z_2) \\ \mathcal{P}(0) = 1 \\ \mathcal{P}^{-1}(z) = \mathcal{P}(-z) \end{cases} \tag{3.11}$$

where the arguments can be both positive and negative. A positive argument, $z > 0$, corresponds to propagation of up-going waves or down-going waves in the dispersive medium, *i.e.*, away from their sources. A negative argument, $-z < 0$, refers to the inverse (resolvent operator) of the operator $\mathcal{P}(z)$, *i.e.*, towards their sources. This operator is of importance in signal restoration since the propagator $\mathcal{P}(-z)$ restores an incident signal $E^+(0,t)$ from a received signal $E^+(z,t)$ by $E^+(0, t - z/c) = [\mathcal{P}(-z)E^+(z,\cdot)](t)$. The rules (3.11) are the requirements for a group; thus, the propagators, $\mathcal{P}(z)$, $-\infty < z < \infty$, form a group.

3.5 Factorization

We now proceed by introducing an appropriate factorization of the wave propagator $\mathcal{P}(z)$. The motivation behind this factorization is to extract the attenuation of the wave front as a separate factor. It is pertinent to factorize the wave propagator as

$$\mathcal{P}(z) = Q(z)\big(1 + P(z;\cdot) *\big) \tag{3.12}$$

[2]We formally see this by the action of a test function $\phi \in C_0^\infty$. Provided a power series expansion exists for ϕ at t we have

$$\begin{aligned} \exp\left(-zc^{-1}\partial_t\right)\phi(t) &= \sum_{n=0}^{\infty} \frac{\left(-zc^{-1}\right)^n}{n!}\phi^{(n)}(t) = \phi(t - z/c) \\ &= \left(\delta(\cdot - z/c) * \phi(\cdot)\right)(t) \end{aligned}$$

[3]In the frequency plane, this wave propagator corresponds to the propagation factor

$$p(z) = \exp\left(-ik(\omega)z\right)$$

where $k(\omega)$ is the complex wave number as a function of angular frequency ω.

where the wave front propagator, $Q(z)$, is the solution of the ordinary differential equation

$$\begin{cases} \partial_z Q(z) = -N(0)Q(z)/c \\ Q(0) = 1 \end{cases}$$

and the solution determines the attenuation of the wave front, *viz.*

$$Q(z) = \exp\left(-\frac{z}{c}N(0)\right)$$

The propagator kernel, $P(z;t)$, satisfies the integro-differential equation

$$\begin{cases} \partial_z P(z;t) = -K(t) - \big(P(z;\cdot) * K(\cdot)\big)(t) \\ P(0;t) = 0 \end{cases} \tag{3.13}$$

which has a unique solution in the space of bounded and smooth functions in each bounded interval, $0 < t < T$, $0 < z < Z$, *cf.* Refs. 25 and 28. $P(z;t)$ vanishes for $t < 0$ since $K(t)$ vanishes for $t < 0$. By definition, the propagator kernels $P(z;t)$ and $P(-z;t)$ are related to one another by the linear Volterra integral equation of the second kind,

$$P(z;t) + P(-z;t) + \left(P(z;\cdot) * P(-z;\cdot)\right)(t) = 0$$

for which a unique solution exists.

The propagator kernel can be expanded in a power series of temporal convolutions that converges in each bounded time interval, $0 < t < T$. We have from equation (3.13)

$$P(z;t) = \sum_{k=1}^{\infty} \frac{(-z)^k}{k!} \left((K*)^{k-1}K\right)(t) \tag{3.14}$$

We use an operator notation which is

$$1 + P(z;\cdot)* = \exp\left(-zK*\right) \tag{3.15}$$

4 The first precursor

The first precursor is defined as the short-time, or wave front, behavior of the impulse response

$$\left[\mathcal{P}(z)\delta\right](t) = Q(z)\left\{\delta(t) + P(z;t)\right\} \tag{4.1}$$

where $\delta(t)$ is the Dirac delta pulse. The first precursor has strong connections to the Green's function or dyadic. We refer to Refs. 5 and 13 for more details on these interrelations.

In the light of (3.13)–(3.14), it makes sense to expand the wave number kernel, $K(t)$, $t > 0$ about $t = 0$. The Maclaurin series of the smooth wave number kernel is

$$\begin{aligned} K(t) =& H(t) \sum_{j=0}^{k-1} \frac{t^j}{j!} \frac{d^j K}{dt^j}(+0) \\ &+ H(t) \int_0^t \frac{(t-t')^{k-1}}{(k-1)!} \frac{d^k K}{dt^k}(t')\, dt' \\ & k = 1, 2, 3, \ldots \end{aligned}$$

where $H(t)$ denotes the Heaviside step function. The time derivatives of the wave number kernel at the origin, $K^{(k)}(+0) = N^{(k+1)}(+0)/c$, $k = 0, 1, 2, 3, \ldots$, are obtained from the recurrence relation

$$\begin{aligned} 2N^{(k)}(+0) =& \frac{\chi_{\mathrm{e}}^{(k)}(+0)}{\epsilon} - \sum_{j=0}^{k-1} N^{(j)}(+0) N^{(k-1-j)}(+0) \\ & k = 1, 2, 3, \ldots \end{aligned}$$

which, in turn, is obtained by differentiating (3.5) with respect to time. For the first coefficients the result is

$$\begin{cases} N(+0) = \dfrac{\chi_{\mathrm{e}}(+0)}{2\epsilon} \\ K(+0) = \dfrac{\chi_{\mathrm{e}}'(+0)}{2c\epsilon} - \dfrac{\chi_{\mathrm{e}}^2(+0)}{8c\epsilon^2} \end{cases}$$

For a simple Debye or Lorentz model, see Section 2, we have

$$\begin{cases} N(+0) = \dfrac{\alpha}{2} > 0 \\ K(+0) = -\dfrac{\alpha}{2c_0\tau} - \dfrac{\alpha^2}{8c_0} < 0 \end{cases} \qquad \text{Debye}$$

and

$$\begin{cases} N(+0) = 0 \\ K(+0) = \dfrac{\omega_p^2}{2c_0} > 0 \end{cases} \qquad \text{Lorentz}$$

Substituting the above expression for $K(t)$ into (3.15) and using (3.12) and the fundamental property of the exponential give

$$\begin{aligned} \mathcal{P}(z) =& Q(z) \exp\left(-zK*\right) \\ =& Q(z) \left(\prod_{j=0}^{k-1} \mathcal{Q}_j(z) \right) \tilde{\mathcal{Q}}_k(z) \end{aligned} \tag{4.2}$$

where the wave front operators are

$$\mathcal{Q}_j(z) = \exp\Big\{-zK^{(j)}(+0)\left(\frac{t^j H(t)}{j!}\right) *\Big\},$$
$$j = 0, 1, 2, \ldots, k-1$$

and the remainder is

$$\begin{aligned}\tilde{\mathcal{Q}}_k(z) = \exp\Big\{&-\frac{z}{(k-1)!} \\ &\times \left(H(t)\int_0^t (t-t')^{k-1} K^{(k)}(t')\,dt'\right) *\Big\}\end{aligned} \tag{4.3}$$

Using the identity $((H*)^n H)(t) = t^n/(n!)H(t)$, the wave front operators can be written in the form

$$\mathcal{Q}_j(z) = 1 + Q_j(z;\cdot)*, \qquad j = 0, 1, 2, \ldots, k-1$$

where the power series of the wave front operators are

$$Q_j(z;t) = H(t)\sum_{i=1}^{\infty}\left(-zK^{(j)}(+0)\right)^i \frac{t^{i(1+j)-1}}{(i(1+j)-1)!i!}$$

The product (4.2) is an exact expansion of the wave propagator. Approximations to the first precursor are obtained by neglecting the remainder (4.3).

4.1 Sommerfeld's forerunner

We are now ready to define the Sommerfeld's forerunner, which is an approximation of the first precursor. Sommerfeld's forerunner at the propagation depth z is

$$\left[\mathcal{P}_{\mathcal{S}}(z)\delta\right](t) = Q(z)\left\{\delta(t) + P_S(z,t)\right\}$$

where the temporal integral operator is defined by taking the first factors in expansion (4.2):

$$\mathcal{P}_S(z) = Q(z)\mathcal{Q}_0(z) = Q(z)\big(1 + P_S(z;\cdot) * \big)$$

Since $Q_0(z;t)$ is a Bessel-function expansion, Sommerfeld's forerunner kernel becomes

$$\begin{aligned}P_S(z;t) = &- zK(+0)\Big[I_0\left(2\sqrt{-zK(+0)t}\right) \\ &- I_2\left(2\sqrt{-zK(+0)t}\right)\Big]H(t) \\ = &- zK(+0)\Big[J_0\left(2\sqrt{zK(+0)t}\right) \\ &+ J_2\left(2\sqrt{zK(+0)t}\right)\Big]H(t)\end{aligned}$$

where I_n and J_n are the modified Bessel function and the Bessel function of order n, respectively. The first formula is appropriate for Debye media ($K(+0) < 0$) and the second for Lorentz media ($K(+0) > 0$). This result, which is a generalization of Sommerfeld's result [29] for the single-resonance Lorentz medium, has been obtained before using various methods [14, 24]. Notice that the forerunner in the Lorentz medium is highly oscillating.

5 The second precursor

The second precursor represents the slowly varying component of the impulse response (4.1). The dominant contribution to this transient is referred to as Brillouin's forerunner. This forerunner is given a precise meaning below.

Here, we seek an expansion of the wave propagator with respect to slowly varying fields. The general idea is to expand the field in terms of its derivatives and neglect the higher-order terms.

Specifically, each smooth field, $E^i(t')$, is expanded in Taylor's formula around the observation time, t:

$$\begin{aligned} E^i(t') = &\sum_{j=0}^{k-1} \frac{(t'-t)^j}{j!} \frac{d^j}{dt^j} E^i(t) \\ &+ \int_t^{t'} \frac{(t'-t'')^{k-1}}{(k-1)!} \frac{d^k}{dt^k} E^i(t'')\, dt'' \\ &k = 1, 2, 3, \ldots \end{aligned}$$

Applying this expansion to the convolution integral $(\chi_{\mathrm{e}} * E^i)(t)$ gives

$$\begin{aligned} \left(\chi_{\mathrm{e}} * E^i\right)(t) = &\sum_{j=1}^{k} \chi_j \frac{d^{(j-1)}}{dt^{(j-1)}} E^i(t) \\ &+ \left(X_k * \frac{d^k}{dt^k} E^i\right)(t) \end{aligned} \tag{5.1}$$

where the coefficients

$$\chi_j = \frac{(-1)^{j-1}}{(j-1)!} \int_0^\infty t^{j-1} \chi_{\mathrm{e}}(t)\, dt \tag{5.2}$$

are proportional to the moments of $\chi_{\mathrm{e}}(t)$ and the remainder is

$$X_k(t) = \frac{(-1)^k}{(k-1)!} H(t) \int_t^\infty (\tau - t)^{k-1} \chi_{\mathrm{e}}(\tau)\, d\tau$$

The convolution in equation (5.1) can be viewed as an expansion of the convolution operator $\chi_{\mathrm{e}}*$. Analogously, the operator $N*$ can be expanded as

$$N* = \sum_{j=1}^{k} n_j \frac{d^{(j-1)}}{dt^{(j-1)}} + N_k * \frac{d^k}{dt^k} \tag{5.3}$$

$$N_k(t) = \frac{(-1)^k}{(k-1)!} H(t) \int_t^\infty (\tau - t)^{k-1} N(\tau)\, d\tau$$

For media such that X_k and N_k tend to zero as k tends to infinity, one can write

$$\chi_{\mathrm{e}} * = \sum_{k=0}^{\infty} \chi_{k+1} \frac{d^k}{dt^k} \delta *, \qquad N * = \sum_{k=0}^{\infty} n_{k+1} \frac{d^k}{dt^k} \delta * \tag{5.4}$$

This is the case for, *e.g.*, Lorentz' model.

The coefficients χ_k and n_k are related to each other. A relation between these coefficients is obtained by inserting the expansions (5.4) in the definition (3.5). The result is

$$\frac{\chi_{k+1}}{\epsilon} = 2n_{k+1} + \sum_{i=0}^{k} n_{k-i+1} n_{i+1}, \quad k = 0, 1, 2, \ldots$$

From this recursion formula, we see that it is sufficient to compute the moments (5.2) of the susceptibility kernel. This approach is particularly advantageous for multiple-resonance media. The coefficients n_k are determined in consecutive order starting with $k = 1$. Explicitly, the first terms are

$$\begin{aligned} n_1 &= \sqrt{1 + \frac{\chi_1}{\epsilon}} - 1, \\ n_2 &= \frac{\chi_2/\epsilon}{2\sqrt{1 + \chi_1/\epsilon}}, \\ n_{k+1} &= \frac{\chi_{k+1}/\epsilon - \sum_{i=1}^{k-1} n_{k-i+1} n_{i+1}}{2(1 + n_1)}, \qquad k > 1 \end{aligned}$$

Using (3.9)–(3.10) and expansion (5.3), the wave propagator, $\mathcal{P}(z)$, $z > 0$, can be written as

$$\begin{aligned} \mathcal{P}(z) &= \exp\left\{ -\frac{z}{c} \frac{d}{dt} \sum_{j=1}^{k} n_j \frac{d^{(j-1)}}{dt^{(j-1)}} \right\} \mathcal{P}_k^r(z) \\ &= \left(\prod_{j=1}^{k} \mathcal{P}_j(z) \right) \mathcal{P}_k^r(z) \end{aligned} \tag{5.5}$$

where

$$\mathcal{P}_j(z) = \exp\left\{ -\frac{z}{c} n_j \frac{d^j}{dt^j} \right\}, \qquad j = 1, 2, 3, \ldots, k$$

and

$$\mathcal{P}_k^r(z) = \exp\left\{ -\frac{z}{c} \frac{d}{dt} N_k * \frac{d^k}{dt^k} \right\}$$

The propagator $\mathcal{P}_j(z)$ are temporal convolution operators:

$$\mathcal{P}_j(z) = P_j(z;\cdot)*, \quad j = 1, 2, 3, \dots, k$$

By definition,

$$P_1(z;t) = \delta\left(t - t_1\right), \quad t_1 = n_1 z/c$$

where the time-delay t_1 is proportional to the propagation distance z.

An expansion of the wave propagator with respect to slowly varying fields can now be obtained. Let $k_B = k_B(\chi_{\rm e})$ be less than or equal to the largest integer such that the moment n_{k_B} satisfies the signature

$$\begin{aligned} n_{4k+1} &\geq 0, \qquad n_{4k+2} \leq 0 \\ n_{4k+3} &\leq 0, \qquad n_{4k+4} \geq 0 \end{aligned}$$

or symbolically

$$\{n_{4k+1}, n_{4k+2}, n_{4k+3}, n_{4k+4}\} = \{+, -, -, +\} \tag{5.6}$$

Provided this numerical signature holds, the kernels $P_j(z;t)$, $j = 2, 3, 4, \dots, k_B$ can be identified as hyper-Airy functions. Fourier transformation reveals that

$$P_j(z;t) = \frac{1}{t_j} B_j\left(\frac{t}{t_j}\right), \quad j = 2, 3, 4, \dots, k_B$$

where the scaling times, t_j, are proportional to the jth root of the propagation depth:

$$t_j = \left(\frac{j|n_j|z}{c}\right)^{\frac{1}{j}}, \qquad j = 1, 2, 3, \dots, k_B$$

Notice that the kernels $P_j(z;t)$, $j = 2, 3, 4, \dots, k_B$ are non-causal. The properties of the infinitely differentiable, bounded, and integrable hyper-Airy functions $B_j(x) := A_j(-x)$ are discussed in Section 9. In particular, $A_2(x)$ is a Gaussian function and $A_3(x)$ is the Airy function $Ai(x)$. Observe that for the Lorentz medium, the Airy function has a negative argument in accordance with known results.

As a consequence of (5.5), the wave propagator, $\mathcal{P}(z)$, can formally be written as

$$\mathcal{P} = P_1 * P_2 * P_3 * P_4 * .... P_{k_B} * \mathcal{P}^r_{k_B} \tag{5.7}$$

for some finite integer k_B. Subject to the above restrictions, for fixed z, the functions $P_j = P_j(z;t)$, $j = 2, 3, 4, \dots, k_B$, are smooth, and since the wave propagator can be written in the form (3.12) where the kernel $P(z;t)$ vanishes for $t < 0$ and is bounded and smooth for $t > 0$, the operator $\mathcal{P}^r_{k_B}(z)$ must produce the highly oscillating field components. In particular, it generates a delta function and Sommerfeld's forerunner

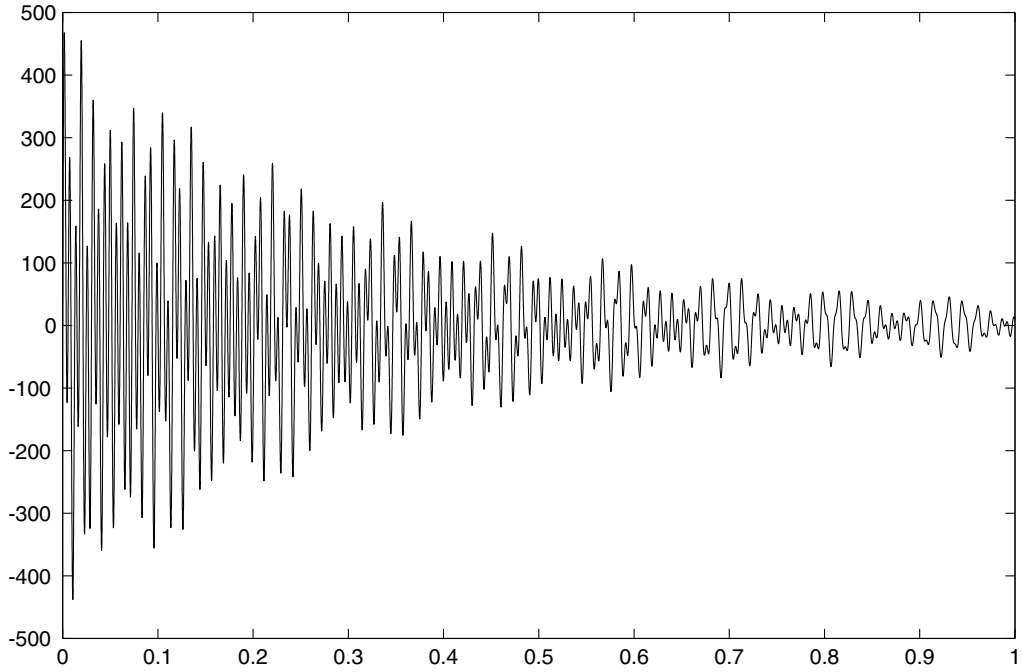

Figure 1: The electric susceptibility kernel, $\chi_{\rm e}(t)/\epsilon$, relevant for the excitation of the ordinary wave, as a function of time, t. Time is measured in units of d/c and the susceptibility kernel is given in units of c/d.

kernel. When we neglect the operator $\mathcal{P}^r_{k_B}(z)$ in the product (5.7) we obtain a more or less accurate approximation to the slowly varying field components.

It is possible to prove that the functions $P_j(z;t)$ satisfy

$$\begin{aligned}
&\int_{-\infty}^{\infty} P_j(z;t)\,dt = 1\\
&\lim_{z\to 0} P_j(z;t) = \delta(t)\\
&P_j(z_1;t) * P_j(z_2;t) = P_j(z_1+z_2;t)
\end{aligned}$$

It is not possible to have arguments $z<0$ in $P_j(z;t)$ when $j>1$ since $P_j(-|z|,t)$ is not a classical function or even a distribution; hence, the inverse to the function $P_j(z;t)$ when $j>1$ does not exist in normal function spaces or in the space of distributions. Thus, for each j, the functions $P_j(z;t)$, $z>0$ form a semi-group in contrast to the entire propagator, $\mathcal{P}(z)$, $-\infty<z<\infty$, that forms a group. Also if we truncate the product in (5.7) at some finite $j>1$ the corresponding propagator does not have an inverse and thus only forms a semi-group.

The theory presented so far holds for the dispersive signature (5.6) only. The numerical example given below indicates that the above method is well suited for normally absorbing resonance (Lorentz) media for which at least $n_1>0$, $n_2<0$, $n_3<0$, but, perhaps, too restricted to be applied to relaxation (Debye) materials for which $n_1>0$, $n_2<0$, but $n_3>0$. In the following, Brillouin's forerunner is defined for materials for which the refractive coefficients n_1, $n_2<0$, and n_3 are finite. The

Debye model indicates that the restriction on the numerical signature (5.6) can be relaxed [13].

5.1 Brillouin's forerunner

Brillouin's forerunner (kernel), $P_B(z;t)$, is defined by

$$P_B = P_1 * P_2 * P_3$$

where $P_j = P_j(z;t)$, and satisfies the parabolic differential equation, see (5.5)

$$\begin{cases} -c\partial_z P_B(z;t) = n_1\partial_t P_B(z;t) \\ \qquad\qquad + n_2\partial_t^2 P_B(z;t) + n_3\partial_t^3 P_B(z;t) \\ P_B(0+0;t) = \delta(t) \end{cases}$$

This definition is essentially the classical, crude approximation to the second precursor in a single-resonance Lorentz material obtained by Brillouin [4]. We get a closed-form expression for Brillouin's forerunner kernel in terms of the Airy function by temporal Fourier transformation technique $Ai(x)$:

$$\begin{aligned} P_B(z;t) = &\exp\left(\frac{n_2^3}{27n_3^2}\frac{z}{c} - \frac{n_2}{3n_3}\left(t - t_B(z)\right)\right) \\ &\times \frac{Ai\left(\mathrm{sign}(n_3)\frac{(t-t_B(z))}{t_3(z)}\right)}{t_3(z)} \end{aligned} \tag{5.8}$$

where the scaling times are

$$t_B(z) = \left(n_1 - \frac{n_2^2}{3n_3}\right)\frac{z}{c}, \qquad t_3(z) = \left(\frac{3|n_3|z}{c}\right)^{\frac{1}{3}}$$

and the sign function is $\mathrm{sign}(n_3) = 1$ for $n_3 > 0$ and $\mathrm{sign}(n_3) = -1$ for $n_3 < 0$. The result (5.8) can also be verified by straightforward differentiation.

As has been pointed out before [23], Brillouin's forerunner (5.8) is valid as an approximation to the slowly varying propagating field in a neighborhood of the quasilatent time $t_B(z)$ only. To obtain better approximations to the "tail" of the second precursor, higher-order approximations must be used. This can be done either by advanced saddle-point analysis [23] or by using the above convolution technique. In this chapter, we employ the latter method. In the numerical examples in Section 6, we find the following expansion to be accurate enough: $P_1 * P_2 * P_3 * P_4 * P_5$.

6 Numerical examples

There are a number of ways to calculate the propagator kernel, $P(z;t)$, in (3.12) numerically by time-domain techniques. One way is to solve the integro-differential

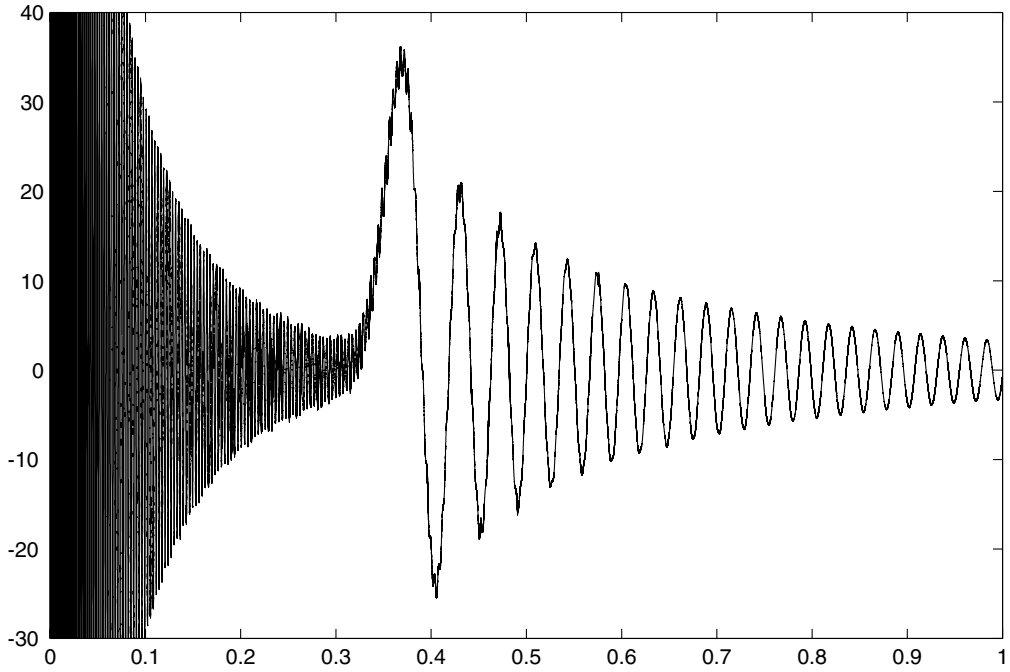

Figure 2: The propagator kernel, $P(d;t)$, relevant for the excitation of the ordinary wave, as a function of time, t. Time is measured in units of d/c and the propagator kernel is given in units of c/d.

equation (3.13) (by integration along the characteristics, z = constant). This is quite time consuming, since a convolution has to be performed at every step in the spatial variable z. For a fixed propagation depth, z, a more efficient way is to solve the following Volterra integral equation of the second kind:

$$\begin{cases} P(z;t) = -\dfrac{1}{t}\left(F(z,\cdot) * P(z;\cdot)\right)(t) - zK(t) \\ F(z,t) = ztK(t) \end{cases} \tag{6.1}$$

This equation can be obtained by Laplace transformation of (3.15) and differentiation with respect to the Laplace transform variable. A straightforward way to solve (6.1) is to discretize the integral by the trapezoidal rule, resulting in a numerical scheme that is very easy to implement. It is also possible to use higher-order integration routines, *e.g.*, the Simpson rule, to get faster convergence. A third time-domain method of calculating $P(z;t)$ is to use the series expansion of the exponential in (3.14). It should be pointed out that the relation

$$\begin{aligned} P(z_1+z_2;t) =& P(z_1;t) + P(z_2;t) \\ &+ \left(P(z_1;\cdot) * P(z_2;\cdot)\right)(t) \end{aligned} \tag{6.2}$$

cf. (3.11), can be utilized in the calculation of $P(z;t)$ in all three cases. In fact, numerical tests indicate that it is necessary to use this rule in order to obtain correct results for large propagation depths.

Ordinary wave			
i	$\lambda_{0_i}^{-1}\,(\mathrm{cm}^{-1})$	$\omega_{p_i}^2/\omega_{0_i}^2$	ν_i/ω_{0i}
1	1227	0.009	0.11
2	1163	0.010	0.006
3	1072	0.67	0.0071
4	797	0.11	0.009
5	697	0.018	0.012
6	450	0.82	0.0090
7	394	0.33	0.007
ϵ=2.356			

Extraordinary wave			
i	$\lambda_{0_i}^{-1}\,(\mathrm{cm}^{-1})$	$\omega_{p_i}^2/\omega_{0_i}^2$	ν_i/ω_{0i}
1	1220	0.011	0.15
2	1080	0.67	0.0069
3	778	0.10	0.010
4	539	0.006	0.04
5	509	0.05	0.014
6	495	0.66	0.0090
7	364	0.68	0.014
ϵ=2.383			

Table 2: Dielectric data quartz in the infrared wavelength region. The notations are: ω_{0i} the resonance frequency ($1/\lambda_{0i} = \omega_{0i}/2\pi c_0$ is given), ω_{p_i} is plasma frequency and ν_i is the collision frequency of the material. The optical response is given by the constant ϵ. Data are from [30].

To illustrate the performance of the technique we apply it to a 7-frequency Lorentz model, *i.e.*, a sum of seven terms given by (2.3), with data given in Table 6. These data has its origin in experimental data [30]. Quartz is not an example of an isotropic material. The material is in fact anisotropic (uniaxial), but provided the optical axis is perpendicular to the direction of propagation, then, for two specific polarizations of the incident field, the reaction is the same as for an isotropic material. These polarizations, which can be excited independently of one another, are known under the names of the ordinary wave and the extraordinary wave.

6.1 Ordinary wave

The ordinary wave is excited provided the magnetic field vector lies in the plane spanned by the optical axis and the direction of propagation. The propagation depth is $z = d = 1$ mm. The relevant electric susceptibility kernel, $\chi_{\mathrm{e}}(t)/\epsilon$, where $\epsilon = 2.356$, as a function of time, t, is depicted in Figure 1. It is convenient to scale time in units of d/c and the susceptibility kernel in units of c/d, where $c = c_0/\sqrt{\epsilon}$. The propagator kernel, $P(d;t)$, as a function of time, t, is depicted in Figure 2.

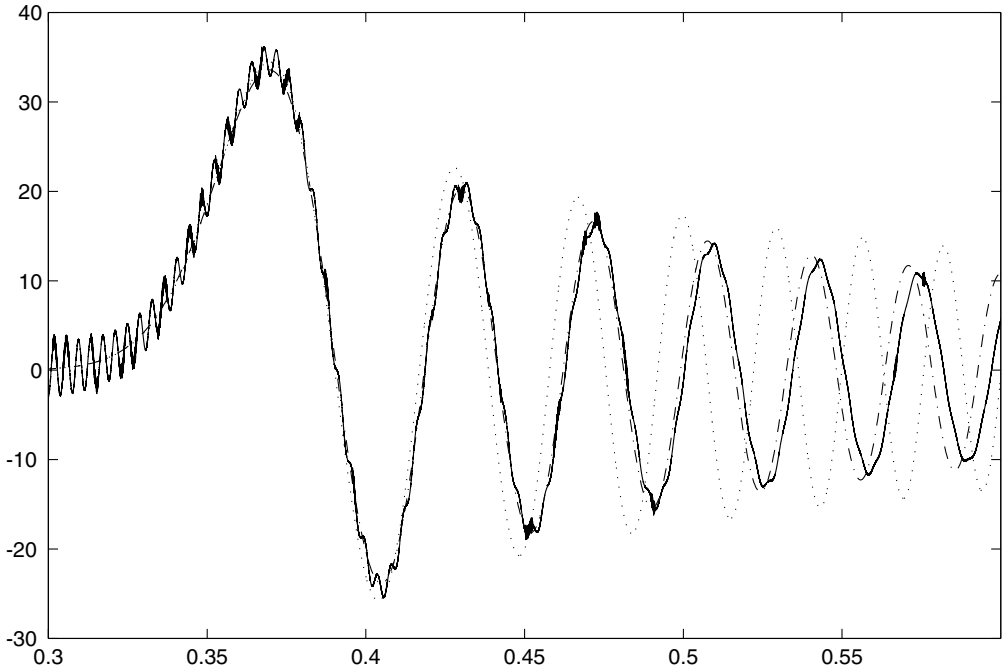

Figure 3: The propagator kernel, $P(d;t)$, and two approximations to the second forerunner, relevant for the excitation of the ordinary wave, as functions of time, t. The solid curve represents the propagator kernel, the dotted curve $(\cdot)$ is the Brillouin approximation to the second forerunner, and the dash-dot curve $(-\cdot)$ represents the improvement of the second forerunner obtained by repeated convolution. Time is measured in units of d/c and the propagator kernel and the approximations are given in units of c/d.

Observe that wave-front time based on the speed $c = c_0/\sqrt{2.356}$ has been used. The result was obtained by solving (6.1) using the trapezoidal rule with 2^{17} and 2^{18} data points followed by a Richardson extrapolation. Furthermore, the propagator rule (6.2) was used three times in both cases. The first five susceptibility coefficients, χ_k/ϵ, measured in $(d/c)^{k-1}$, the refractive coefficients, n_k, measured in $(d/c)^{k-1}$, and the scaling times, t_k, measured in d/c, relevant for the ordinary wave, can be found in Table 3. Observe that the signature holds for these refractive coefficients. The propagator kernel, $P(d;t)$, and two approximations to the second forerunner, as functions of time, t, are depicted in Figure 3. In this time interval, the Brillouin's forerunner, given by the formula (5.8), constitutes a fairly good first approximation to the forerunner kernel. However, it cannot predict the behavior of the "tail" of the signal correctly, neither with respect to phase nor to amplitude. The second approximation, which is the numerical result of the convolution of the functions $P_k(d;t)$, $k = 1, 2, 3, 4, 5$, clearly improves this "tail" significantly.

Responses to other excitations are obtained by convolution:

$$g(t) + (g(\cdot) * P(d;\cdot))(t)$$

where $g(t)$ is the given excitation at $z = 0$ and the use of wave-front time is un-

	Ordinary wave		
	χ_k/ϵ	n_k	t_k
$k=1$	8.3488964e-01	3.5458098e-01	3.5458098e-01
$k=2$	-1.2811896e-05	-4.7290994e-06	3.0754185e-03
$k=3$	-3.1858282e-06	-1.1759542e-06	1.5223128e-02
$k=4$	1.1902902e-10	3.9830254e-11	3.5527796e-03
$k=5$	1.6950985e-11	5.7466086e-12	7.7924913e-03

	Extraordinary wave		
	χ_k/ϵ	n_k	t_k
$k=1$	9.1355434e-01	3.8331281e-01	3.8331281e-01
$k=2$	-2.0288013e-05	-7.3331255e-06	3.8296542e-03
$k=3$	-3.9186225e-06	-1.4164100e-06	1.6197081e-02
$k=4$	2.3902811e-10	7.8888404e-11	4.2147158e-03
$k=5$	2.4317709e-11	8.0649325e-12	8.3390034e-03

Table 3: Dimensionless susceptibility coefficients, χ_k/ϵ, refractive coefficients, n_k, and scaling times, t_k, relevant for the ordinary and the extraordinary waves. The signature holds also for these excitations.

derstood. Excitations of particular interest are the Heaviside step function, $H(t)$, and a sinusoidal function terminated at one end, *i.e.*, $H(t)\sin(2\pi ft)$, where f is the frequency. The responses to these signals are found in Figure 4 and Figure 5, respectively. In the latter case, the frequency $f = 1$ THz has been chosen. The trapezoidal rule has been employed in the numerical integrations. Richardson extrapolation has been used in these two cases. Observe that the first precursor in Figure 4 is of much lower amplitude than in Figure 2, due to cancellations at the integration, and that it almost vanishes in Figure 5 (cancellation of the order of 10^7). Observe also that the excitations are clearly distinguishable in the responses in both cases, although time shifts have occurred, and that the signals are built up surprisingly quickly.

6.2 Extraordinary wave

The extraordinary wave is excited provided the electric field vector lies in the plane spanned by the optical axis and the direction of propagation. The propagation depth is $d = 1$ mm also in this example. The relevant electric susceptibility kernel, $\chi_{\rm e}(t)/\epsilon$, where $\epsilon = 2.383$, as a function of time, t, is depicted in Figure 6. The susceptibility kernel is presented in units of c/d, where $c = c_0/\sqrt{\epsilon}$ and time is measured in units of d/c and they consequently differ from the one used in case of the ordinary wave. The propagator kernel, $P(d;t)$, as a function of time, t, is depicted in Figure 7. Observe that wave-front time based on the speed $c = c_0/\sqrt{2.383}$ has been used. The result has been obtained using Richardson extrapolation with the number of data points 2^{18} and 2^{17}, and the propagator rule (6.2) was used three times in both cases. The first five susceptibility coefficients, χ_k/ϵ, measured in $(d/c)^{k-1}$, the refractive coefficients,

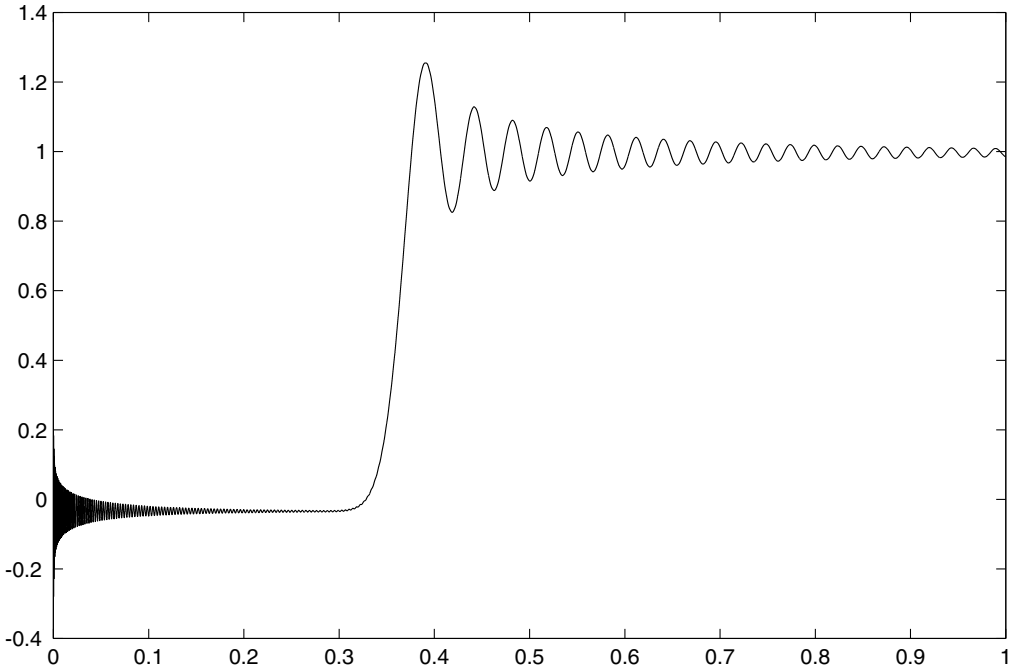

Figure 4: The step response, $H(t) + (H(\cdot) * P(d;\cdot))(t)$, when the ordinary wave is excited. The propagator kernel, $P(d;t)$, is depicted in Figure 2. Wave-front time measured in units of d/c is used.

n_k, measured in $(d/c)^{k-1}$, and the scaling times, t_k, measured in d/c, relevant for the extraordinary wave, are shown in Table 3. The signature for these refractive coefficients holds for this excitation also. The propagator kernel, $P(d;t)$, and two approximations to the second forerunner, as functions of time, t, are depicted in Figure 8. Similar to the case of the ordinary wave, Brillouin's forerunner, given by the formula (5.8), constitutes a fairly good first approximation to the forerunner kernel, but cannot predict the behavior of the "tail" of the signal correctly. The second approximation is the numerical result of the convolution of the functions $P_k(d;t)$, $k = 1, 2, 3, 4, 5$, and improves the result significantly.

7 Scattering by a slab

The analysis in Section 3 which was used in the investigation of the first and the second precursors in Sections 4 and 5, was made under the assumption that the medium was homogeneous in the whole space. This situation is, of course, non-physical since no measurements can be made inside the material. A physically more realistic situation is to let the wave interact with the dispersive material in a finite slab. The measurement and the effects of the first and the second precursors are then observed in the transmitted or reflected field [5]. In this section, the alterations in the analysis in this physically more realistic case are analyzed.

A general, linearly polarized plane wave impinges normally on a temporally

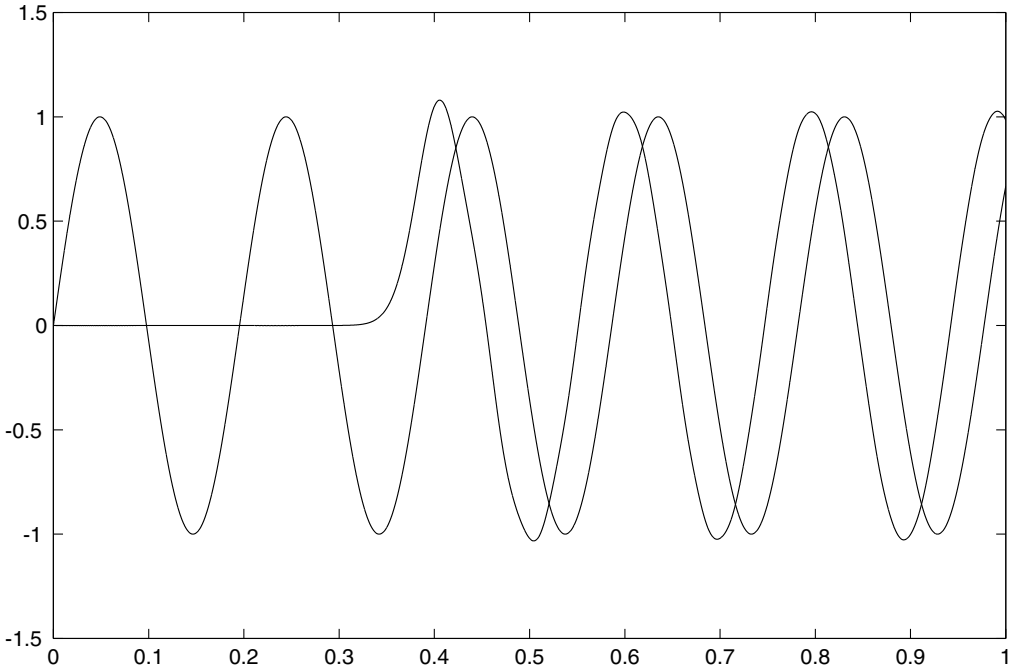

Figure 5: A sinusoidal terminated at one end, $H(t)\sin(2\pi ft)$, where $f = 1$ THz, and the response of this signal, $H(t)\sin(2\pi ft) + (H(\cdot)\sin(2\pi f\cdot) * P(d;\cdot))(t)$, when the ordinary wave is excited. The propagator kernel, $P(d;t)$, is depicted in Figure 2. Wave-front time measured in units of d/c is used.

dispersive slab, $0 < z < d$, see Figure 9. For the sake of simplicity, the medium is assumed to be located in vacuum and $\epsilon = \mu = 1$ in the medium, *i.e.*, no optical response. As seen from above, the optical response can always be introduced by a suitable limit process. The incident plane wave at the front wall, $z = 0$, at time t is given by

$$\begin{cases} \boldsymbol{E}^i(t) = \boldsymbol{e}_x E^i(t) \\ \boldsymbol{H}^i(t) = \boldsymbol{e}_y H^i(t) \end{cases}$$

where $H^i(t) = E^i(t)/\eta_0$. The incident electric field, $E^i(t)$, is assumed to be bounded, smooth, and initially quiescent, *i.e.*, it vanishes for $t < 0$. All electromagnetic fields in the slab are assumed to be initially quiescent.

The back edge $z = d$ can either be finite for a slab of finite thickness, or it could be infinite (large enough so there are no effects from reflections at the back edge) to model a half space problem. Both these situations are analyzed in this chapter.

The reflected plane wave at the front wall, $z = 0$, at time t is given by

$$\begin{cases} \boldsymbol{E}^r(t) = \boldsymbol{e}_x E^r(t) \\ \boldsymbol{H}^r(t) = \boldsymbol{e}_y H^r(t) \end{cases}$$

where $H^r(t) = -E^r(t)/\eta_0$.

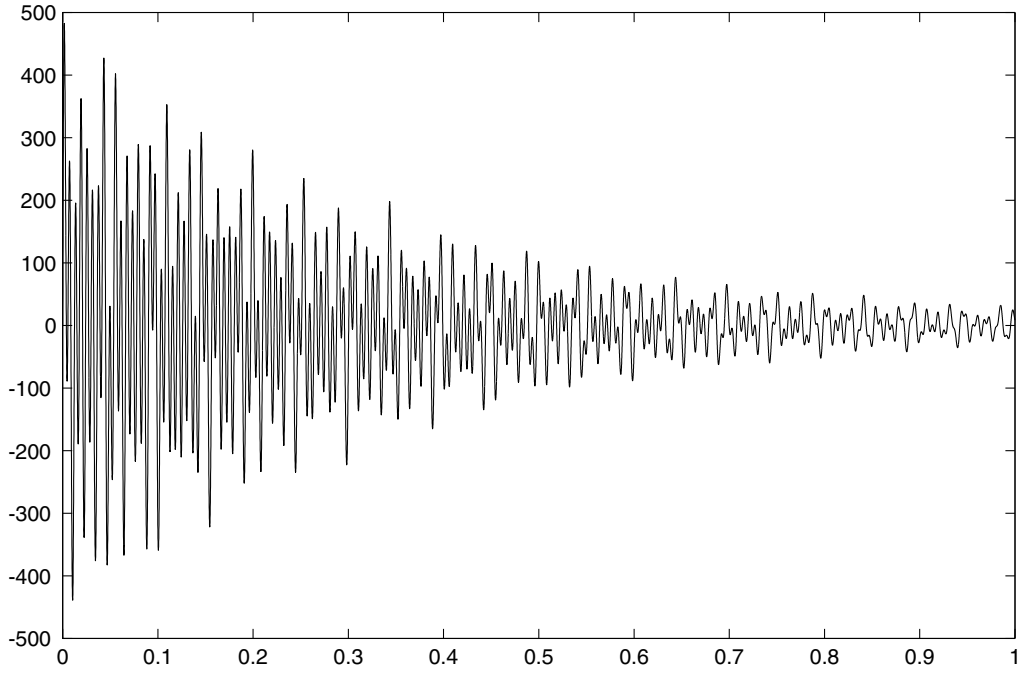

Figure 6: The electric susceptibility kernel, $\chi_{\rm e}(t)/\epsilon$, relevant for the excitation of the extraordinary wave, as a function of time, t. Time is measured in units of d/c and the susceptibility kernel is given in units of c/d.

Analogously, the transmitted plane wave at the rear wall, $z = d$, at time t is

$$\begin{cases} \boldsymbol{E}^t(t) = \boldsymbol{e}_x E^t(t) \\ \boldsymbol{H}^t(t) = \boldsymbol{e}_y H^t(t) \end{cases}$$

where $H^t(t) = E^t(t)/\eta_0$. In terms of these scattered waves, the boundary conditions are

$$\begin{cases} E^i(t) + E^r(t) = E(0+0,t) \\ H^i(t) + H^r(t) = H(0+0,t) \end{cases} \\ \begin{cases} E^t(t) = E(d-0,t) \\ H^t(t) = H(d-0,t) \end{cases} \tag{7.1}$$

where the argument $0+0$ and $d-0$ denote the limit values from above at $z = 0$ and from below at $z = d$, respectively.

An application of the Duhamel's principle shows that there is a linear relation between the reflected and the transmitted fields and the incident field, respectively, [8]. We have

$$\begin{cases} E^r(t) = \left[\mathcal{R}E^i\right](t) = \displaystyle\int_{-\infty}^{t} R(t-t')E^i(t')\,dt' \\ E^t(t+d/c_0) = Q(d)E^i(t) + \displaystyle\int_{-\infty}^{t} T(t-t')E^i(t')\,dt' \end{cases} \tag{7.2}$$

where $R(t)$ and $T(t)$ are the reflection and the transmission kernels of the slab, respectively.

7.1 Half-space problem

The introduction of the relative intrinsic impedance of the temporally dispersive medium promotes simple, natural definitions of reflection and transmission operators for the electric field at normal incidence at a (single) non-dispersive–dispersive interface ($d \to \infty$). The reflection operator viewed from the non-dispersive medium is defined by $\mathcal{R} = \mathcal{R}_\infty = (\mathcal{Z}+1)^{-1}(\mathcal{Z}-1)$ and relates the reflected field to the incident one. This temporal integral operator can be written in the form

$$\mathcal{R}_\infty \equiv R_\infty *$$

where the kernel $R_\infty(t)$ depends on time only and vanishes for $t < 0$. The reflection kernel $R_\infty(t)$ satisfies the Volterra integral equations of the second kind [13]

$$\begin{cases} 2R_\infty(t) - Z(t) + (Z * R_\infty)(t) = 0 \\ 2R_\infty(t) + N(t) + (N * R_\infty)(t) = 0 \\ 4R_\infty(t) + 2(\chi_\mathrm{e} * R_\infty)(t) + \chi_\mathrm{e}(t) \\ \qquad\qquad + (\chi_\mathrm{e} * (R_\infty * R_\infty))(t) = 0 \end{cases}$$

These equations imply that $R_\infty(t)$ is bounded, smooth, and continuously dependent on data for $t > 0$. According to the first two equations, $R_\infty(t)$ is the resolvent kernel of $N(t)/2$ and $-R_\infty(t)$ is the resolvent kernel of $Z(t)/2$. The third equation is recognized as the imbedding equation for the semi-infinite dispersive medium [1].

Since the reflection operator for the up-going electric field is $\mathcal{R}_\infty$, the reflection operator for the down-going electric field is $-\mathcal{R}_\infty$. The transmission operator for the up-going electric field is then

$$\mathcal{T} = 1 + \mathcal{R}_\infty$$

and the transmission operator for the down-going electric field $1 - \mathcal{R}_\infty$. The solution of the propagation problem is then

$$E^+(z) = (1 + \mathcal{R}_\infty)\mathcal{P}(z)(\delta_{z/c} * E^i)$$

and $E^-(z) = 0$ for $z > 0$. The total electric and magnetic fields in the medium are

$$\begin{cases} E(z) = (1 + \mathcal{R}_\infty)\mathcal{P}(z)(\delta_{z/c} * E^i) \\ \eta H(z) = (1 - \mathcal{R}_\infty)\mathcal{P}(z)(\delta_{z/c} * E^i) \end{cases}$$

7.2 Scattering problem

Recall that the split fields do not couple. Suppressing the general time-dependence,

$$\begin{cases} E^\pm(z) := E^\pm(z,t) \\ E^i := E^i(t) \\ E^r := E^r(t) \\ E^t := E^t(t) \end{cases} \tag{7.3}$$

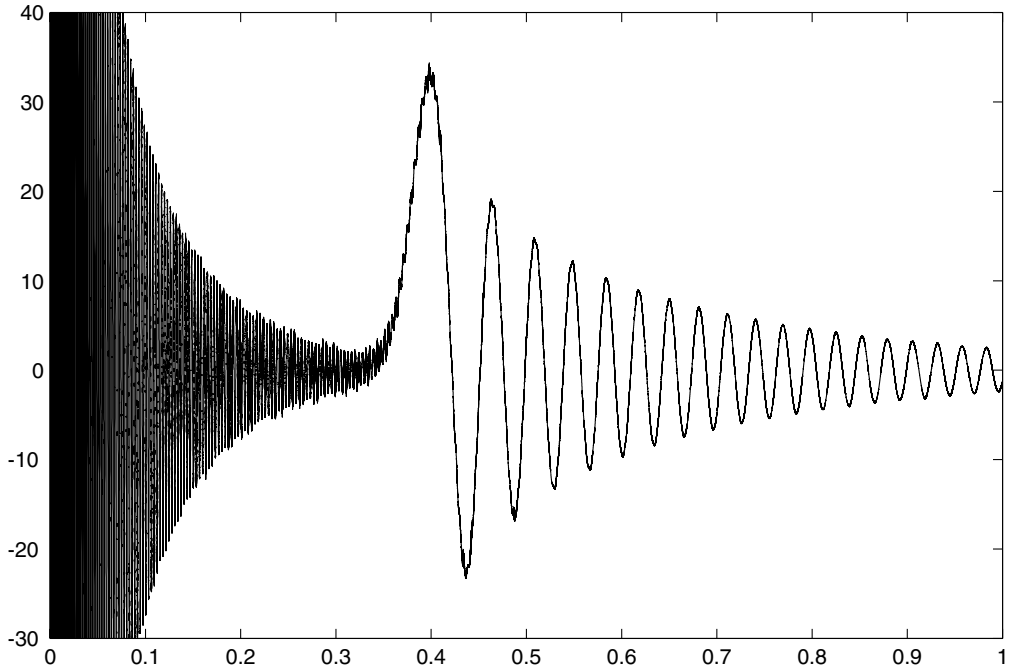

Figure 7: The propagator kernel, $P(d;t)$, relevant for the excitation of the extraordinary wave, as a function of time, t. Time is measured in units of d/c and the propagator kernel is given in units of c/d.

the boundary conditions (7.1) at $z = 0$ and at $z = d$ reduce to

$$\begin{aligned} \begin{pmatrix} E^i \\ E^r \end{pmatrix} &= \begin{pmatrix} \mathcal{S} & \mathcal{S}\mathcal{R}_\infty \\ \mathcal{S}\mathcal{R}_\infty & \mathcal{S} \end{pmatrix} \begin{pmatrix} E^+(0) \\ E^-(0) \end{pmatrix} \\ \begin{pmatrix} E^t \\ 0 \end{pmatrix} &= \begin{pmatrix} \mathcal{S} & \mathcal{S}\mathcal{R}_\infty \\ \mathcal{S}\mathcal{R}_\infty & \mathcal{S} \end{pmatrix} \begin{pmatrix} E^+(d) \\ E^-(d) \end{pmatrix} \end{aligned} \tag{7.4}$$

respectively, where the temporal integral operator

$$\mathcal{S} \equiv 1 + S*, \qquad \mathcal{S}\mathcal{T} = 1 \quad (\mathcal{S} = \mathcal{T}^{-1})$$

is the inverse (resolvent operator) of the transmission operator $\mathcal{T} \equiv 1 + R_\infty *$. The kernel of $\mathcal{S}$ is $S(t) = N(t)/2$.

Suppressing the general time-dependence as in (7.3), (3.7) gives

$$\begin{cases} E^+(z) = \mathcal{P}(z)E^+(0) \\ E^-(z) = \mathcal{P}(d-z)E^-(d) \end{cases}$$

Upon setting $z = d$ in the first equation and $z = 0$ in the second equation, the boundary conditions (7.4) can be exploited, and the four unknown functions $E^\pm(0)$, $E^\pm(d)$ eliminated. Straightforward calculations show that the solution of the direct scattering problem reads

$$\begin{cases} E^t = \mathcal{M}(1 - \mathcal{R}_\infty^2)\mathcal{P}(d)(\delta_{d/c} * E^i) \\ E^r = \mathcal{R}_\infty E^i - \mathcal{M}(1 - \mathcal{R}_\infty^2)\mathcal{R}_\infty\mathcal{P}(2d)(\delta_{2d/c} * E^i) \end{cases}$$

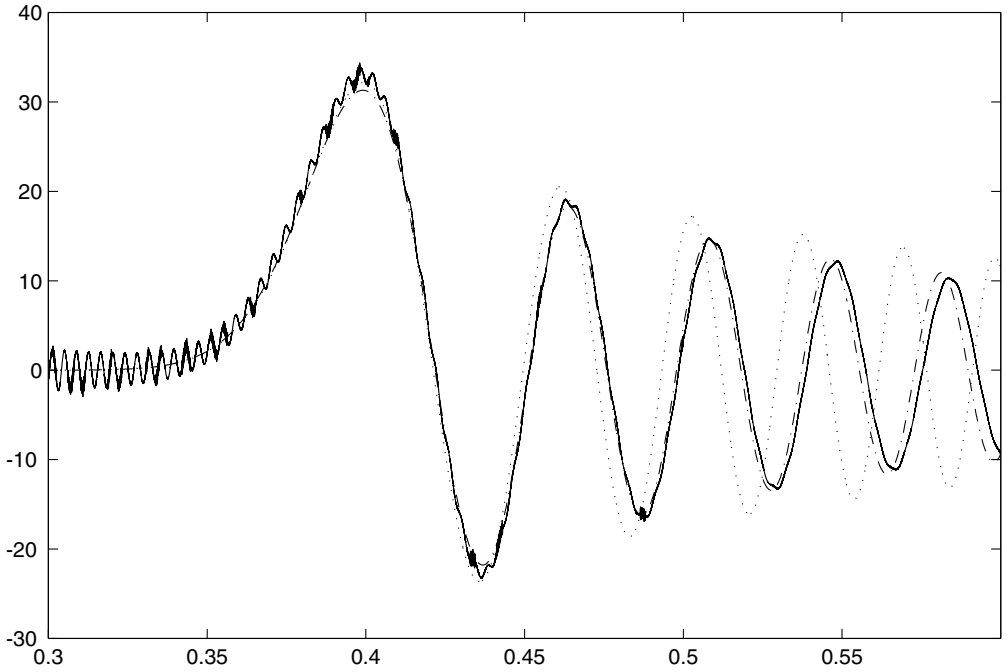

Figure 8: The propagator kernel, $P(d;t)$, and two approximations to the second forerunner, relevant for the excitation of the extraordinary wave, as functions of time, t. Time is measured in units of d/c and the propagator kernel and the approximations are given in units of c/d. As in the previous example, the solid curve represents the propagator kernel, the dotted curve $(\cdot)$ is the Brillouin approximation to the second forerunner, and the dash-dot curve $(-\cdot)$ represents the improvement of the second forerunner obtained by repeated convolution.

where the temporal integral operator

$$\mathcal{M} = \left(1 - \mathcal{R}_\infty^2 \mathcal{P}(2d)\delta_{2d/c} * \right)^{-1}$$

represents multiple propagation through the slab, and the notation $(\delta_a * E^i)(t) := E^i(t-a)$ for time-shift has been employed. From these integral equations relating $R(t)$, R_∞, $T(t)$ and $P(z;t)$ can be obtained. For the internal electric fields, the result is

$$\begin{cases} E^+(z) = \mathcal{M}\mathcal{T}\mathcal{P}(z)(\delta_{z/c} * E^i) \\ E^-(z) = -\mathcal{M}\mathcal{T}\mathcal{R}_\infty\mathcal{P}(2d-z)(\delta_{(2d-z)/c} * E^i) \end{cases}$$

Observe that these relations easily can be affirmed heuristically.

A propagation problem closely related to the present one is the internal source problem, where an initially quiescent, transverse current distribution, $\boldsymbol{e}_x J_x(z,t)$, excites the medium, $0 < z < d$.

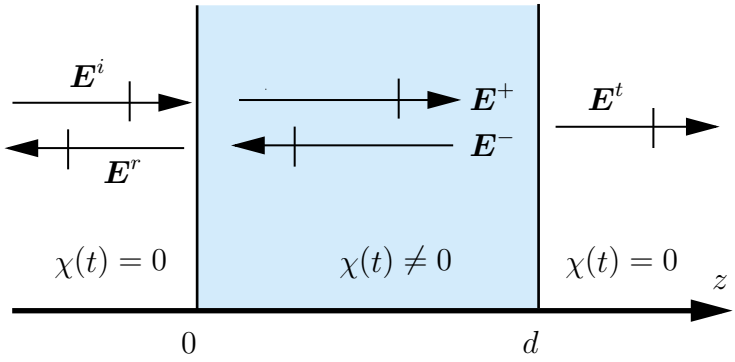

Figure 9: The scattering geometry with the incident, scattered, and internal electric fields indicated.

8 Biisotropic media

As an example illustrating the difficulties that appear when analyzing complex materials, we choose the homogeneous bi-isotropic material. The simplest way to analyze wave propagation problems in such materials is to introduce the complex electromagnetic field.

The use of complex field vectors in order to write the free-space Maxwell equations in a more economical form has been proposed by several authors, see, e.g., Stratton [31]. The basic idea is to define a complex field vector such that the real part represents the electric field and the imaginary part the magnetic field, or *vice versa*, and such that the Maxwell equations decouple. The first ideas along these lines seem to be due to Beltrami [2]. In time-harmonic analysis, these fields or generalizations of these fields are referred to as Beltrami fields [22], wave fields [20], self-dual fields [20], or Bohren fields [18]. Wave fields have been used with success in the analysis of monochromatic wave propagation phenomena in linear bi-isotropic materials, see, e.g., Lindell *et al.* [20]. Related work, that can be applied to general linear materials, can be found in [19], where not only Beltrami fields, but also Beltrami induction fields, are introduced.

The constitutive relations of a linear, homogeneous, bi-isotropic material that is invariant under time translations, can be written in the form

$$c_0\eta_0\boldsymbol{D} = \varepsilon\boldsymbol{E} + \xi\eta_0\boldsymbol{H}, \qquad c_0\boldsymbol{B} = \zeta\boldsymbol{E} + \mu\eta_0\boldsymbol{H} \tag{8.1}$$

where the *relative* permittivity and permeability operators of the medium are

$$\varepsilon = 1 + \chi_{\rm ee}(t)*, \qquad \mu = 1 + \chi_{\rm mm}(t)*$$

the *relative* cross-coupling operators

$$\xi = \chi_{\rm em}(t)*, \qquad \zeta = \chi_{\rm me}(t)*$$

Observe that ε, μ, ξ, and ζ now denote operators, and they differ slightly from the ones used in Section 2.

These constitutive relations are general enough, since optical responses always can be introduced afterwards, see above. Two special kinds of bi-isotropic materials are widely discussed in the literature, namely, reciprocal, isotropic chiral (or Pasteur) media, which satisfy the relation $\chi_{\mathrm{me}}(t) = -\chi_{\mathrm{em}}(t)$, and isotropic, non-reciprocal, achiral (or Tellegen) materials, for which the relation $\chi_{\mathrm{me}}(t) = \chi_{\mathrm{em}}(t)$ holds [20]. It is well known—although once doubted—that there are Pasteur materials, both natural and man-made, whereas the existence of Tellegen materials, or, more generally, non-reciprocal bi-isotropic materials has been doubted, although the evidence for this has not been convincing.

Substituting the constitutive relations, (8.1), into the Maxwell equations, (2.1), gives a linear system of first-order hyperbolic integro-differential equations in the electric and magnetic field vectors only:

$$\begin{cases} \nabla \times \boldsymbol{E} = -c_0^{-1}\partial_t \left(\zeta \boldsymbol{E} + \mu\eta_0 \boldsymbol{H}\right), \\ \nabla \times \eta_0 \boldsymbol{H} = \eta_0 \boldsymbol{J} + c_0^{-1}\partial_t \left(\varepsilon \boldsymbol{E} + \xi\eta_0 \boldsymbol{H}\right) \end{cases} \tag{8.2}$$

The aim is to decouple this system of equations by a linear change of variables.

8.1 Complex time-dependent electromagnetic fields

An arbitrary (real-valued) time-dependent electromagnetic field $\{\boldsymbol{E}(\boldsymbol{r},t), \boldsymbol{H}(\boldsymbol{r},t)\}$ in a linear, homogeneous, bi-isotropic medium can be represented uniquely by a complex field vector, $\boldsymbol{Q}(\boldsymbol{r},t)$, (and its complex conjugate, $\boldsymbol{Q}^*(\boldsymbol{r},t)$,) as

$$\begin{cases} \boldsymbol{E} = \boldsymbol{Q} + \boldsymbol{Q}^*, \\ \eta_0 \boldsymbol{H} = i\mathcal{Y}\boldsymbol{Q} - i\mathcal{Y}^*\boldsymbol{Q}^* \end{cases} \tag{8.3}$$

where the complex-valued temporal integral operator

$$\mathcal{Y} = 1 + Y(t) *$$

is the relative intrinsic admittance of the medium and $\mathcal{Y}^*$ its complex conjugate. The imaginary unit is denoted by i. The inverse of the transformation (8.3) is

$$\boldsymbol{Q} = \frac{1}{2}\mathcal{Z}\left(\mathcal{Y}^*\boldsymbol{E} - i\eta_0 \boldsymbol{H}\right) \tag{8.4}$$

where the real-valued temporal integral operator

$$\mathcal{Z} = 1 + Z(t) *$$

is a relative intrinsic impedance defined by

$$\left(\mathcal{Y} + \mathcal{Y}^*\right)\mathcal{Z}/2 = 1 \tag{8.5}$$

Obviously, considering units the field vectors $\boldsymbol{Q}(\boldsymbol{r},t)$ and $\boldsymbol{Q}^*(\boldsymbol{r},t)$ can be interpreted as complex electric fields.

The introduction of the complex electromagnetic field vector reduces the system of integro-differential equations (8.2) to the first-order, dispersive wave equation

$$\nabla \times \boldsymbol{Q} = -ic_0^{-1}\partial_t \mathcal{N}\, \boldsymbol{Q} - i\eta_0 \mathcal{Z}\boldsymbol{J}/2 \tag{8.6}$$

where the complex-valued temporal integral operator

$$\mathcal{N} = 1 + N(t) *$$

is referred to as the index of refraction. It is understood that $\mathcal{Y}$, $\mathcal{N}$, and $\mathcal{Z}$ are intrinsic operators of the medium, that is, independent of the field vectors. Below, equation (8.6) is referred to as the wave-field equation.

8.2 Intrinsic operators

The decoupling of the Maxwell equations leads to conditions on the relative intrinsic admittance and the index of refraction in terms of the susceptibility operators of the bi-isotropic medium:

$$\mathcal{N} = \mu\mathcal{Y}^* + i\xi, \qquad \mathcal{N}\mathcal{Y}^* = \varepsilon - i\zeta\mathcal{Y}^*$$

Combining these equations gives

$$(\mathcal{N} - i\xi)(\mathcal{N} + i\zeta) = \mu\varepsilon, \qquad \mu\mathcal{Y} = \mathcal{N}^* + i\xi \tag{8.7}$$

with solutions

$$\begin{cases} \mathcal{N} = i\dfrac{\xi - \zeta}{2} + \sqrt{\mu\varepsilon - \dfrac{(\xi+\zeta)^2}{4}}, \\ \mu\mathcal{Y} = i\dfrac{\xi + \zeta}{2} + \sqrt{\mu\varepsilon - \dfrac{(\xi+\zeta)^2}{4}} \end{cases}$$

where the positive square-root operator has been chosen:

$$\sqrt{\mu\varepsilon - \frac{(\xi+\zeta)^2}{4}} = 1 + N_{\mathrm{co}}(t) *$$

Here, the real-valued integral kernel $N_{\mathrm{co}}(t)$ satisfies the nonlinear Volterra integral equation of the second kind

$$\begin{aligned} &2N_{\mathrm{co}}(t) + (N_{\mathrm{co}} * N_{\mathrm{co}})(t) \\ &= \chi_{\mathrm{ee}}(t) + \chi_{\mathrm{mm}}(t) + (\chi_{\mathrm{ee}} * \chi_{\mathrm{mm}})(t) - (\chi * \chi)(t) \end{aligned}$$

where $\chi(t) = (\chi_{\mathrm{em}}(t) + \chi_{\mathrm{me}}(t))/2$ is the non-reciprocity kernel. Volterra integral equations of the second kind are uniquely solvable in the space of of continuous functions in each compact time-interval and the solutions depend continuously on data [15, 21]. Consequently, the kernel $N_{\mathrm{co}}(t)$ inherits causality and smoothness properties from the susceptibility kernels. Straightforward analysis shows that a

choice of the negative square-root operator does not add or alter anything of significance for the present discussion.

In terms of the kernel $N_{\rm co}(t)$ and the chirality kernel $\kappa(t) = (\chi_{\rm em}(t) - \chi_{\rm me}(t))/2$, the complex-valued refractive kernel becomes

$$N(t) = N_{\rm co}(t) + i\kappa(t)$$

Clearly, the refractive kernel of the bi-isotropic medium is real if and only if the medium is Tellegen, that is, $\kappa(t) = 0$. Similarly, the admittance kernel can be written as

$$Y(t) = Y_{\rm co}(t) + iY_{\rm cross}(t)$$

where the components $Y_{\rm co}(t)$ and $Y_{\rm cross}(t)$ are real-valued functions. The second identity (8.7) implies that the admittance kernel satisfies the linear Volterra integral equation of the second kind

$$Y(t) + (Y * \chi_{\rm mm})(t) = N_{\rm co}(t) - \chi_{\rm mm}(t) + i\chi(t)$$

In particular, the admittance kernel inherits causality and smoothness properties from the susceptibility kernels. Unique solubility gives that the admittance kernel of the bi-isotropic medium is real if and only if the medium is Pasteur, that is, $\chi(t) = 0$. Finally, the impedance kernel $Z(t)$ satisfies a linear Volterra integral equation of the second kind:

$$Z(t) + (Z * N_{\rm co})(t) = \chi_{\rm mm}(t) - N_{\rm co}(t)$$

This follows from equation (8.5). The impedance kernel inherits causality and smoothness properties from the susceptibility kernels.

In summary, by introducing the complex field vector (8.4), the Maxwell equations for the linear, homogeneous, bi-isotropic medium (8.2) reduce to the first-order dispersive wave equation (8.6). The refractive, admittance, and impedance kernels in equations (8.3) and (8.6) depend on the susceptibility kernels of the medium only. Obtaining these intrinsic kernels of the medium, of which the first two are complex and the third is real, is a well posed problem. Specifically, Volterra integral equations of the second kind are solved. The final result, the wave equation (8.6), is an appropriate starting point for discussing pulse propagation phenomena in bi-isotropic materials and scattering from such materials.

8.3 Transverse electric and magnetic (TEM) pulses in an unbounded bi-isotropic medium

A current distribution of the form

$$\boldsymbol{J}(\boldsymbol{r}, t) = \boldsymbol{J}_T(\boldsymbol{r}, t) = \boldsymbol{e}_x J_x(z, t) + \boldsymbol{e}_y J_y(z, t)$$

gives rise to TEM waves in the medium:

$$\boldsymbol{Q}(\boldsymbol{r}, t) = \boldsymbol{Q}_T(\boldsymbol{r}, t) = \boldsymbol{e}_x Q_x(z, t) + \boldsymbol{e}_y Q_y(z, t)$$

This Ansatz reduces the wave-field equation (8.6) to

$$\partial_z \boldsymbol{Q} = ic_0^{-1}\partial_t \mathcal{N}\boldsymbol{e}_z \times \boldsymbol{Q} + i\eta_0 \mathcal{Z}\boldsymbol{e}_z \times \boldsymbol{J}/2$$

We introduce the wave splitting

$$\begin{aligned}\boldsymbol{E}_+^{\pm} =& \frac{1}{2}\left(\boldsymbol{Q} \mp i\,\boldsymbol{e}_z \times \boldsymbol{Q}\right)\\ =& \left(\boldsymbol{e}_x \mp i\,\boldsymbol{e}_y\right)\left(Q_x \pm i\,Q_y\right)/2 \equiv \left(\boldsymbol{e}_x \mp i\,\boldsymbol{e}_y\right)E_+^{\pm}\end{aligned}$$

which decomposes the total electric right-hand circularly polarized (RCP) field, $\boldsymbol{Q}$, into an up-going RCP field, $\boldsymbol{E}_+^+$, and a down-going RCP field, $\boldsymbol{E}_+^-$ such that $\boldsymbol{Q} = \boldsymbol{E}_+^+ + \boldsymbol{E}_+^-$. The wave equations for the amplitudes of these waves, $E_+^{\pm} = (Q_x \pm iQ_y)/2$, are

$$\partial_z E_+^{\pm} = \mp c_0^{-1}\partial_t \mathcal{N} E_+^{\pm} \mp \eta_0 \mathcal{Z} J_+^{\pm}/2 \tag{8.8}$$

where $J_+^{\pm} = (J_x \pm i\,J_y)/2$.

Similarly, the total electric left-hand circularly polarized (LCP) field, $\boldsymbol{Q}^*$, can be split into an up-going LCP field, $\boldsymbol{E}_-^+$, and a down-going LCP field, $\boldsymbol{E}_-^-$ such that $\boldsymbol{Q}^* = \boldsymbol{E}_-^+ + \boldsymbol{E}_-^-$. These fields are

$$\begin{aligned}\boldsymbol{E}_-^{\pm} =& \left(\boldsymbol{E}_+^{\pm}\right)^*\\ =& \frac{1}{2}\left(\boldsymbol{Q}^* \pm i\,\boldsymbol{e}_z \times \boldsymbol{Q}^*\right) \equiv \left(\boldsymbol{e}_x \pm i\,\boldsymbol{e}_y\right)E_-^{\pm}\end{aligned}$$

where the amplitudes of the LCP fields, $E_-^{\pm} = (E_+^{\pm})^* = \left(Q_x^* \mp i\,Q_y^*\right)/2$, satisfy the wave equations

$$\partial_z E_-^{\pm} = \mp c_0^{-1}\partial_t \mathcal{N}^* E_-^{\pm} \mp \eta_0 \mathcal{Z} J_-^{\pm}/2$$

where $J_-^{\pm} = (J_+^{\pm})^* = (J_x \mp i\,J_y)/2$. Consequently, the total electric field in the bi-isotropic medium can be written as the sum of the up-going and the down-going electric RCP and LCP fields:

$$\begin{aligned}\boldsymbol{E} =& \left(\boldsymbol{e}_x - i\,\boldsymbol{e}_y\right)E_+^+ + \left(\boldsymbol{e}_x + i\,\boldsymbol{e}_y\right)E_+^-\\ &+ \left(\boldsymbol{e}_x + i\,\boldsymbol{e}_y\right)E_-^+ + \left(\boldsymbol{e}_x - i\,\boldsymbol{e}_y\right)E_-^-\end{aligned}$$

The total magnetic field is

$$\begin{aligned}\eta_0\boldsymbol{H} =& i\mathcal{Y}\left(\boldsymbol{e}_x - i\,\boldsymbol{e}_y\right)E_+^+ + i\mathcal{Y}\left(\boldsymbol{e}_x + i\,\boldsymbol{e}_y\right)E_+^-\\ &- i\mathcal{Y}^*\left(\boldsymbol{e}_x + i\,\boldsymbol{e}_y\right)E_-^+ - i\mathcal{Y}^*\left(\boldsymbol{e}_x - i\,\boldsymbol{e}_y\right)E_-^-\end{aligned}$$

8.4 Normal incidence on a slab

Combining the complex field vector concept with the wave splitting technique decomposes the propagation problem into two subproblems: (i) solve the dispersive wave equations (8.8) and (ii) obtain scattering relations at the plane interfaces using the boundary conditions. The techniques used for obtaining propagators and forerunners for isotropic media presented above apply also to the bi-isotropic case in this section. The only difference is that the refractive index now is complex resulting in complex propagators and forerunners.

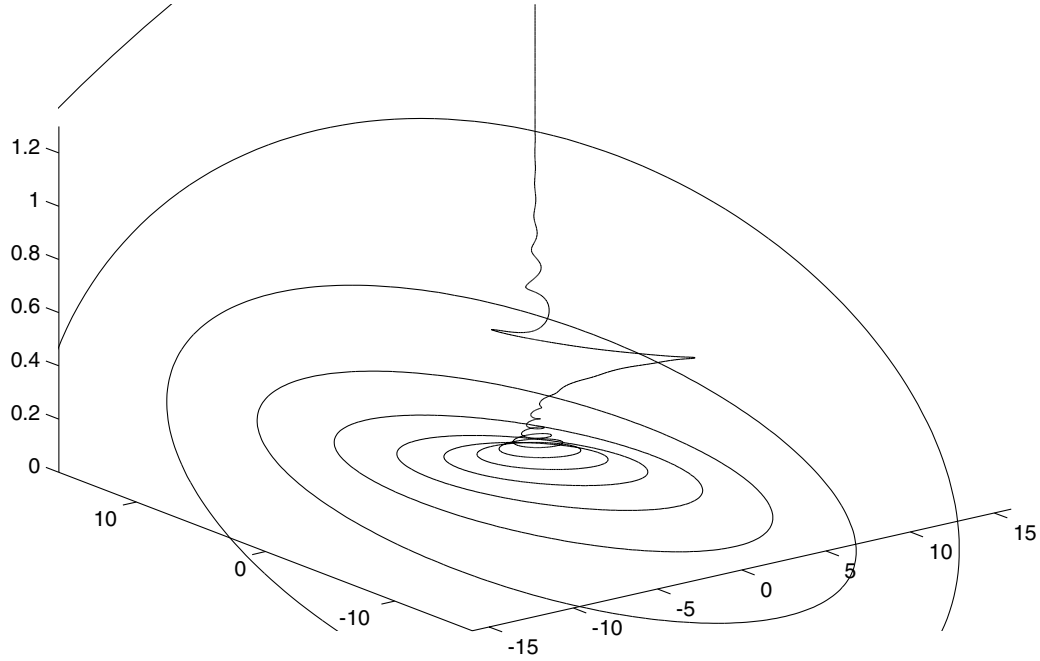

Figure 10: The response of an isotropic, chiral medium, at $z = d$, to an electric delta pulse excitation, at $z = 0$, polarized in the x-direction. The curve $(\mathrm{Re}\, Q(d)P(d;t), \mathrm{Im}\, Q(d)P(d;t), t)$, where the direction of increasing time, t, is upwards, and $Q(d)P(z;t)$ is the complex propagator kernel corresponding to the complex propagator kernel, $N(t)$, has been plotted. Time is measured from the arrival of the wave front and in units of d/c_0. The propagator kernel is given in units of c_0/d.

8.5 Numerical example

Figure 10 shows the response of a non-magnetic isotropic, chiral medium, at $z = d$, to an electric delta pulse excitation, at $z = 0$, polarized in the x-direction. Specifically, the parameterized curve $\{\mathrm{Re}\, Q(d)P(d;t), \mathrm{Im}\, Q(d)P(d;t), t\}$ is depicted, where the direction of increasing time, t, is upwards, and $Q(d)P(z;t)$ is the complex propagator kernel corresponding to the complex refractive kernel, $N(t)$. Results on wave propagation in this particular medium have been presented in [6] in a different way. Specifically, the medium is characterized by the single-resonance Condon-model parameters $\omega_p = \omega_0 = 100 \times c_0/d$, $\nu = 20 \times c_0/d$, and $\alpha = -0.001 \times d/c_0$, see [6]. The second forerunner is clearly distinguishable as an irregularity in the spiral curve, starting approximately at $t = 0.4d/c_0$, and ending approximately at $t = 1.2d/c_0$. For $d = 10^{-6}$ m, the values of parameters ω_p, ω_0, and α coincide with the ones used in [32].

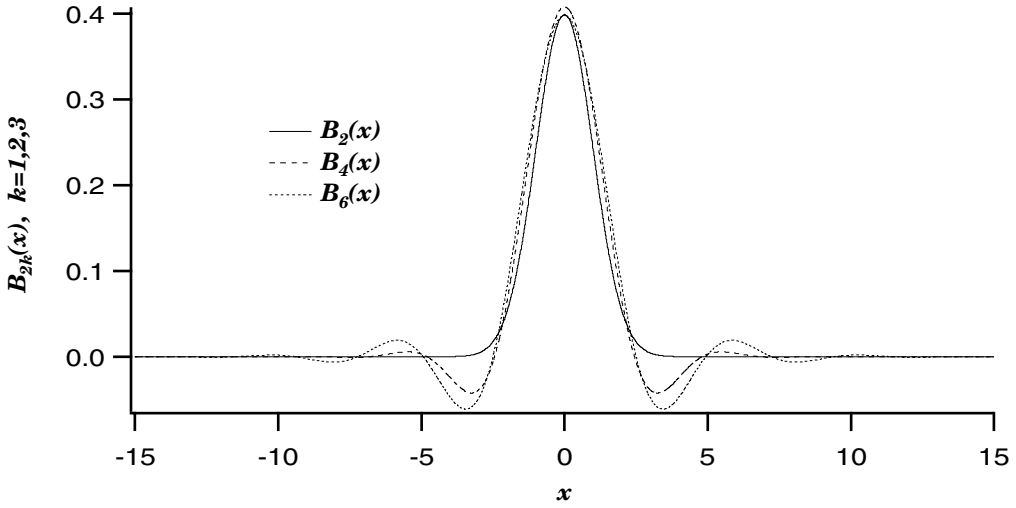

Figure 11: The Hyper-Airy functions $B_{2k}(x)$ for $k = 1, 2, 3$.

9 Hyper-Airy functions A_k and B_k

In this section, we examine the hyper-Airy functions $A_{2k}(x)$, $-\infty < x < +\infty$ in some detail. Let k be an arbitrary positive integer. The real function $A_{2k}(x)$ of real argument x is the inverse Fourier transform of the function $\exp(-\xi^{2k}/(2k))$. The real function $A_{2k+1}(x)$ of real argument x is the inverse Fourier transform of the function $\exp(i\xi^{2k+1}/(2k+1))$.

The hyper-Airy functions $A_{2k}(x)$ of even indices belong to the Schwartz class of rapidly decreasing functions $\mathcal{S}$, that is, the set of all $\phi \in \mathcal{C}^\infty$ such that

$$\sup_{x\in\mathbb{R}} |x^\beta \phi^{(\alpha)}(x)| < \infty$$

for all non-negative integers α and β. Thus, in particular, the functions $A_{2k}(x)$ are bounded, infinitely differentiable, and integrable. Moreover, these functions are even functions of x. Explicitly,

$$A_{2k}(x) = \frac{1}{2\pi}\int_{-\infty}^{\infty} e^{-\xi^{2k}/(2k)+ix\xi}\, d\xi, \quad x \in \mathbb{R}$$

The hyper-Airy functions $A_{2k+1}(x)$ of odd indices belong to the Schwartz class of tempered distributions $\mathcal{S}'$, that is, the continuous linear forms on $\mathcal{S}$. The generalized functions $A_{2k+1}(x)$ coincide with the bounded, infinitely differentiable, and integrable functions

$$A_{2k+1}(x) = \frac{1}{2\pi}\int_{-\infty+i\eta}^{\infty+i\eta} e^{i\zeta^{2k+1}/(2k+1)+ix\zeta}\, d\zeta, \; x \in \mathbb{R} \tag{9.1}$$

where η is an arbitrary positive constant. Equation (9.1) provides integral representations for the hyper-Airy functions $A_{2k+1}(x)$ of odd indices. The leading behaviors

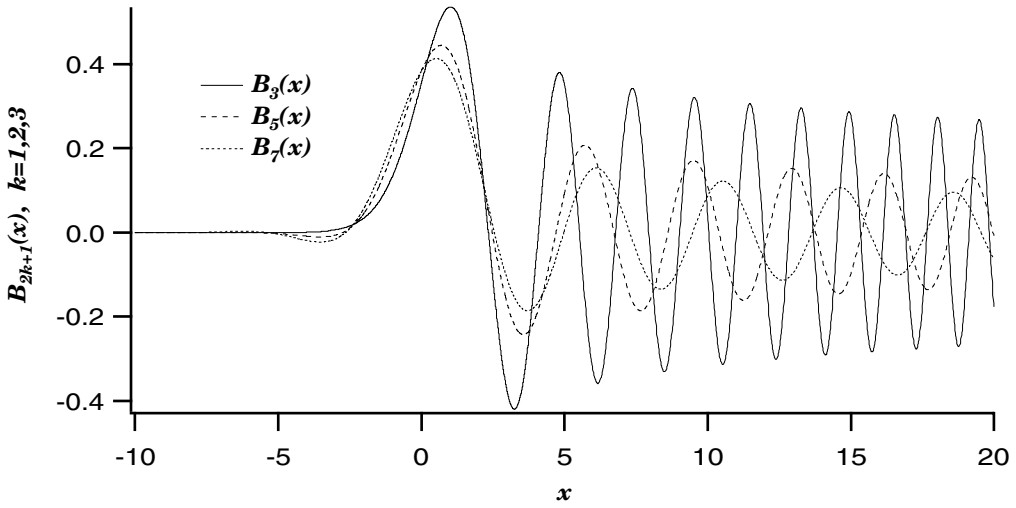

Figure 12: The Hyper-Airy functions $B_{2k+1}(x)$ for $k = 1, 2, 3$.

of $A_{2k+1}(x)$ as $x \to -\infty$ show that these functions do not belong to the Schwartz class $\mathcal{S}$ [13].

By the definition of A_k as an inverse Fourier transform we get

$$\int_{-\infty}^{\infty} A_k(x)\, dx = 1.$$

Furthermore, $A_2(x)$ is a Gaussian function and $A_3(x)$ is the Airy function $Ai(x)$. We have

$$\begin{cases} A_2(x) = \dfrac{1}{\sqrt{2\pi}} e^{-x^2/2} \\ A_3(x) = Ai(x) \end{cases} \quad x \in \mathbb{R}$$

Differentiating under the integral sign yields the ordinary differential equations

$$\begin{cases} A_{2k}^{(2k-1)}(x) = (-1)^k x A_{2k}(x) \\ A_{2k+1}^{(2k)}(x) = (-1)^{k+1} x A_{2k+1}(x) \end{cases} \quad x \in \mathbb{R}$$

for the hyper-Airy functions. These equations, which are higher-order generalizations of the Airy equation,

$$Ai''(x) = x Ai(x), \quad x \in \mathbb{R}$$

are sometimes referred to as hyper-Airy equations.

In summary, the hyper-Airy functions of even indices are even, oscillating functions, which are exponentially attenuated for large arguments. The leading behavior of the hyper-Airy functions of odd indices are oscillating and exponentially attenuated for large positive arguments. The leading behavior of the hyper-Airy functions of odd indices are oscillating but only weakly attenuated for large negative arguments. The frequencies, the phase angles, and attenuating functions can be obtained explicitly in each separate case [13].

9.1 The functions $B_k(x)$

When Brillouin's forerunner is to be discussed, it is more appropriate to introduce the functions $B_k(x)$, defined as the hyper-Airy functions evaluated at a negative argument, *i.e.*, $B_k(x) := A_k(-x)$. The functions $B_k(x)$, $k = 2, 3, 4, 5, 6, 7$ are plotted in Figure 11 and Figure 12.

References

[1] R. S. Beezley and R. J. Krueger. An electromagnetic inverse problem for dispersive media. *J. Math. Phys.*, **26**(2), 317–325, 1985.

[2] E. Beltrami. Considerazioni idrodinamiche. *Rend. Inst Lombardo Acad. Sci. Lett.*, **22**, 122–131, 1889.

[3] L. Brillouin. Über die Fortpflanzung des Lichtes in dispergierenden Medien. *Ann. Phys.*, **44**, 203–240, 1914.

[4] L. Brillouin. *Wave propagation and group velocity.* Academic Press, New York, 1960.

[5] I. Egorov. Second forerunners in reflection and transmission data. *J. Opt. A: Pure Appl. Opt.*, **1**, 51–59, 1999.

[6] I. Egorov and S. Rikte. Forerunners in bigyrotropic materials. *J. Opt. Soc. Am. A*, **15**(9), 2391–2403, 1998.

[7] J. Fridén, G. Kristensson, and A. Sihvola. Effect of dissipation on the constitutive relations of bi-anisotropic media–the optical response. *Electromagnetics*, **17**(3), 251–267, 1997.

[8] P. R. Garabedian. *Partial Differential Equations.* Chelsea Publishing Company, New York, 1986.

[9] M. Gustafsson. *Inverse Electromagnetic Scattering Problems — A Time-Domain Optimization Approach.* Licentiate thesis, Lund Institute of Technology, Department of Electromagnetic Theory, P.O. Box 118, S-211 00 Lund, Sweden, 1998.

[10] S. He, S. Ström, and V. H. Weston. *Time Domain Wave-splittings and Inverse Problems.* Oxford University Press, Oxford, 1998.

[11] J. D. Jackson. *Classical Electrodynamics.* John Wiley & Sons, New York, third edition, 1999.

[12] A. Karlsson and G. Kristensson. Constitutive relations, dissipation and reciprocity for the Maxwell equations in the time domain. Technical Report

LUTEDX/(TEAT-7005)/1–35/(1989), Lund Institute of Technology, Department of Electromagnetic Theory, P.O. Box 118, S-211 00 Lund, Sweden, 1989. Short published version *J. Electro. Waves Applic.*, **6**(5/6), 537–551 (1992).

[13] A. Karlsson and S. Rikte. The time-domain theory of forerunners. *J. Opt. Soc. Am. A*, **15**(2), 487–502, 1998.

[14] A. Karlsson and R. Stewart. Wave propagators for transient waves in periodic media. *J. Opt. Soc. Am. A*, **12**(7), 1513–1521, 1995.

[15] R. Kress. *Linear Integral Equations*. Springer-Verlag, Berlin Heidelberg, 1989.

[16] G. Kristensson. Direct and inverse scattering problems in dispersive media—Green's functions and invariant imbedding techniques. In R. Kleinman, R. Kress, and E. Martensen, editors, *Direct and Inverse Boundary Value Problems*, Methoden und Verfahren der Mathematischen Physik, Band 37, pages 105–119, Frankfurt am Main, 1991. Peter Lang.

[17] G. Kristensson. Time-domain methods for complex media. In W. S. Weiglhofer, editor, *BIANISOTROPICS'97*, pages 119–124, Department of Mathematics, University of Glasgow, Great Britain, 1997.

[18] A. Lakhtakia, V. K. Varadan, and V. V. Varadan. *Time-Harmonic Electromagnetic Fields in Chiral Media*, volume 335 of *Lecture Notes in Physics*. Springer-Verlag, New York, 1989.

[19] A. Lakhtakia. Time-dependent Beltrami fields in material continua: The Beltrami-Maxwell postulates. *Int. J. Infrared and MM Waves*, **15**(2), 369–394, 1994.

[20] I. V. Lindell, A. H. Sihvola, S. A. Tretyakov, and A. J. Viitanen. *Electromagnetic Waves in Chiral and Bi-isotropic Media*. Artech House, Boston, London, 1994.

[21] P. Linz. *Analytical and Numerical Methods for Volterra Equations*. SIAM, Philadelphia, 1985.

[22] S. A. Maksimenko, G. Y. Slepyan, and A. Lakhtakia. Gaussian pulse propagation in a linear, lossy chiral medium. *J. Opt. Soc. Am. A*, **14**(4), 894–900, 1997.

[23] K. E. Oughstun and G. C. Sherman. *Electromagnetic Pulse Propagation in Causal Dielectrics*. Springer-Verlag, Berlin Heidelberg, 1994.

[24] S. Rikte. Sommerfeld's forerunner in stratified isotropic and bi-isotropic media. Technical Report LUTEDX/(TEAT-7036)/1–26/(1994), Lund Institute of Technology, Department of Electromagnetic Theory, P.O. Box 118, S-211 00 Lund, Sweden, 1994.

[25] S. Rikte. Existence, uniqueness, and causality theorems for wave propagation in stratified, temporally dispersive, complex media. *SIAM J. Math. Anal.*, **10**, 1997.

[26] S. Rikte. The theory of the propagation of TEM-pulses in dispersive bi-isotropic slabs. *Wave Motion*, **29**(1), 1–21, January 1999.

[27] J. Robert L. Ochs and G. Kristensson. Using local differential operators to model dispersion in dielectric media. *J. Opt. Soc. Am. A*, **15**(8), 2208–2215, 1998.

[28] T. M. Roberts. Causality theorems. In J. P. Corones, G. Kristensson, P. Nelson, and D. L. Seth, editors, *Invariant Imbedding and Inverse Problems*. SIAM, 1992.

[29] A. Sommerfeld. Über die Fortpflanzung des Lichtes in dispergierenden Medien. *Ann. Phys.*, **44**, 177–202, 1914.

[30] W. G. Spitzer and D. A. Kleinman. Infrared lattice bands of quartz. *Phys. Rev.*, **121**(5), 1324–1335, 1961.

[31] J. A. Stratton. *Electromagnetic Theory*. McGraw-Hill, New York, 1941.

[32] P. G. Zablocky and N. Engheta. Transients in chiral media with single-resonance dispersion. *J. Opt. Soc. Am. A*, **10**(4), 740–758, 1993.